Accepted Manuscript

Quarterly Journal of Engineering Geology and Hydrogeology

A cluster-based multiparametric similarity test for the compartmentalization of crystalline rocks into structural domains

Attoumane Abi, Julien Walter, Ali Saeidi & Romain Chesnaux

DOI: https://doi.org/10.1144/qjegh2021-136

To access the most recent version of this article, please click the DOI URL in the line above. When citing this article please include the above DOI.

Received 28 September 2021
Revised 1 December 2021
Accepted 21 December 2021

A cluster-based multiparametric similarity test for the compartmentalization of crystalline rocks into structural domains

Attoumane Abi[1*], Julien Walter[1], Ali Saeidi[1], Romain Chesnaux[1]

[1] *Université du Québec à Chicoutimi, Department of Applied Sciences, Chicoutimi, Québec G7H 2B1, Canada*

ORCID ID: AA, 0000-0002-3398-403X; JW, 0000-0003-2514-6180

Present addresses: AA, Université du Québec à Chicoutimi, Department of Applied Sciences, Chicoutimi, Québec G7H 2B1, Canada

*Corresponding author (e-mail: attoumane.abi1@uqac.ca)

Abstract: Usually, fracture sampling studies comprise the collection of several fracture samples, which involve many fracture clusters. Grouping fracture samples into structural domains is generally useful for geologists, hydrogeologists, and geomechanicians as a region of fractured rocks is subdivided into sub-regions with similar behavior in terms of their hydromechanical properties. One of the common methods used for grouping fracture samples into structural domains considers the fracture orientation of clusters and ignores several fracture parameters, such as fracture spacing, aperture, and persistence, which are important for fluid circulation in the rock mass.

In this study, we proposed a new cluster-based similarity method that considered the orientation of clusters as well as clusters' aperture, persistence, and fracture spacing. Field investigations were conducted in the Grenville geological province of the Canadian Shield in the Lanaudière region, Quebec, Canada, where fractures were sampled from 30 outcrops and four boreholes. The proposed method is more suitable than other methods, and has applications in hydrogeology, rock mechanics, and especially in studies of fluid circulation in the rock mass. In addition, a method for the compartmentalization of a given study area into structural domains by means of Voronoi diagrams was also proposed.

Supplementary material: [description of material] is available at https://doi.org/xxxx.

For the purposes of this paper, it is useful to define some frequently used keywords. A fracture sample is a subset of a fracture population within a given study area. A fracture sample is usually composed of fractures from the same sampling station. Several fracture samples may come from the same fracture population, but adding up the fracture samples doesn't yield the fracture population. The term "fracture samples" is sometimes shortened to "sample" for readability.

It is well established that fracture networks play a significant role in promoting fluid flow in the rock mass (Hamm *et al.* 2007; Scesi and Gattinoni 2012). Because crystalline rocks have negligible primary permeability (permeability of the rock matrix) in comparison to their secondary permeability (permeability due to fractures), fracture characterization commonly represents one of the most important steps for determining the hydraulic characteristics of the rock mass (Singhal and Gupta 2010; Roques *et al.* 2014). Fracture characterization generally requires several fracture samples, which can be from different data sources, such as outcrops, tunnels and boreholes (Singhal and Gupta 2010). In a given study area with many fracture samples, geologists tend to compartmentalize the study area into structurally homogeneous subareas by comparing and grouping fracture samples. Those homogeneous subareas are called structural domains (Miller 1983; Kulatilake *et al.* 1990).

The notion of structural domains can be traced back to the early 1900s when the foundations of modern structural petrology was emerging in Austria through the work of Bruno Sander and collaborators (Turner *et al.* 1963). Back then, a structural domain was defined as a statistically homogeneous section of the rock mass with regard to a given structural element (e.g., fracture, foliation) at a particular scale (Turner *et al.* 1963). Sensu stricto, a structurally homogeneous rock body would be identical in all structural elements that compose the rock mass; however, such a phenomenon is rare in nature (Turner *et al.* 1963). Delineating structural domains is the first step in studying the hydromechanical behavior of a rock mass (Kulatilake *et al.* 1990). Structural domains are also essential in hydrological studies as the hydraulic properties of the geological formation may vary between different domains (Kulatilake *et al.* 1990).

From the definition, it can be inferred that several structural elements may be used in the process of defining structural domains (Turner *et al.* 1963). Generally, depending on the investigated geological processes, researchers may use fold and foliation data (Turner *et al.* 1963; Vollmer 1990) to determine structural domains, and fracture data is also used (Miller 1983; Martin and Tannant 2004;

Song *et al.* 2015; Guo *et al.* 2020), especially in engineering fields. Independently of the considered structural element, the orientation of the structural element is the main characteristic that is utilized to explore homogeneity and delimit the domains (Turner *et al.* 1963).

Generally, major structural elements such as faults, folds, weathering effects, volcanic vents, and mineralized zones constitute the boundaries of structural domains (Turner *et al.* 1963; Priest 1993). However, there are conditions where major structural elements are very limited (Li *et al.* 2014b). In such circumstances, an analysis of structural elements such as fracture samples and foliation data may be sufficient to delineate the domains, as introduced by Miller (1983) and Vollmer (1990), respectively.

In studies involving the hydromechanical behavior of the rock mass, structural domains are derived from fracture data. Early statistical methods were proposed by Miller (1983) and Mahtab and Yegulalp (1984) for the assessment of the homogeneity of fracture samples by comparing pairs of fracture samples with one another. Those methods are especially useful when stereographic plots of fracture orientations are distributed in ways that do not allow an efficient comparison of fracture samples (Kulatilake *et al.* 1990; Phi 2016).

Miller's method consists of subdividing the stereonet into several equal-area patches and comparing the number of fracture poles that fall into corresponding patches between the two fracture samples that are being compared. In order to assess the homogeneity of the compared samples, Miller (1983) used the chi-square test to evaluate whether there is a statistically significant difference between the stereonets of the samples. The main limitations of Miller's method are that the subdivision of the stereonets into equal area patches is arbitrary, and different patch design may lead to different results (Miller 1983). Because of the enumerated limitations and that orientation is the only fracture parameter that Miller (1983) used, several researchers have proposed variants of his method. These variants involved other equal area subdivision patches of the stereonet (QuocPhi *et al.* 2012; Song *et al.* 2015), other fracture parameters (Li et al., 2015; Song et al., 2015, 2018;

Zhang et al., 2016; Zhou et al., 2018), or other statistical tests (Martin and Tannant 2004; Li *et al.* 2014a, 2015; Song *et al.* 2015, 2018). In the literature, it was noted that Miller's test and its variants were mainly used in engineering studies, which did not exceed a few square kilometers.

Mahtab and Yegulalp (1984) developed a method based on fracture orientations known as a similarity test. This method had a different approach, in which fracture clusters (or fracture sets) were compared between two adjacent fracture samples; however, their method was only justifiable when fracture poles on the stereonet formed clusters and were not randomly distributed. A fracture cluster is a group of fractures that share the same characteristics within a fracture sample. Two adjacent samples are considered to be of the same structural domain when they share at least one similar fracture cluster (Mahtab and Yegulalp 1984; Kulatilake *et al.* 1997). From adjacent samples, the assessment of the similarity between clusters is based on the acute angle between clusters' resultant vectors (i.e. the acute angle between mean poles) (Mahtab and Yegulalp 1984).

While Mahtab and Yegulalp (1984) considered only fracture orientation in their method, several researchers (Zhou and Maerz 2002; Tokhmechi *et al.* 2011; Liu *et al.* 2020) proved that the use of multiple fracture parameters made clustering more accurate. Using only fracture orientations in the similarity test may lead to inaccuracies in judging the similarity between clusters from two adjacent samples. To illustrate this, in a simulated fracture sample composed of eight clusters, Tokhmechi et al. (2011) identified only three clusters when fracture orientation was alone considered. However, all eight clusters were identified when fracture orientation, infilling material, and infilling percentage parameters were considered and the principal component analysis was adopted.

Although many methods of assessing the homogeneity of fracture samples exist, none of them is based on the similarity of clusters with regard to a set of fracture parameters that control the fluid circulation in the rock mass. This study proposes a new cluster-based method for defining and delimiting structural domains by taking into consideration the fracture orientation, aperture, spacing, and persistence (also called fracture size) in the similarity analysis of clusters from adjacent

samples. Fracture orientation influences fluid direction, fracture aperture influences the flow through fractures, and fracture spacing and persistence influence fracture density and interconnectivity, which in return impact the capacity of the rock mass to transmit water (Scesi and Gattinoni 2010; Wenli *et al.* 2019). This method is based on the Mahtab and Yegulalp (1984) similarity test and further explores testing the similarity of clusters with regard to fracture spacing, persistence, and aperture.

To illustrate the developed methodology, a study site with accessible outcrops of crystalline rocks and non-exploited boreholes was selected for fracture samples. Fieldwork was conducted in Lanaudière, an administrative region located in the southern part of the province of Quebec, Canada. The data was collected under the scope of the project PACE-Lanaudière (Programme d'acquisition de connaissances sur les eaux souterraine), which aims to map the groundwater resources of Lanaudière. The application of the proposed method led to the compartmentalization of the study area into homogeneous structural domains with distinct hydrogeological properties. Such compartmentalization is particularly useful for building large-scale groundwater models in crystalline rocks, which takes into consideration the heterogeneity of different fracture networks in the study area.

Study area

The study area is bounded by the Sainte-Julienne Fault in the north-west, the river Maskinongé in the north, the Saint-Cuthbert Fault in the south-east, and the river Bayonne in the south-west (Figure 1). Two main geological provinces are found in the study area, namely, the Grenville Province and the Saint-Laurent Platform (Béland 1967; Clark and Globensky 1976). The Saint-Laurent Platform is composed of sedimentary rocks and occupies less than 14% of the study area. The remaining 86% is occupied by the Grenville Province, which is located in the southeastern part of the Canadian shield and is mainly composed of Precambrian metamorphic and igneous rocks (Rivers *et al.* 1989).

The data used in this study is collected in the Grenville Province. In this area specifically, the Saint-Didace granite, charnockitic granulite, and hornblende-biotite-plagioclase gneisses are the most common types of rocks. Saint-Didace granites are characterized by coarse-grained pinkish-gray porphyroid type of granite, with large feldspar grains (Béland 1967). Charnockitic granulites are composed of sodic-calcic plagioclase, orthoclase, perthitic microline, diopsidic clinopyroxene, green hornblende, and biotite (Béland, 1967). The hornblende-biotite-plagioclase gneisses are medium to coarse-grained rocks with black hornblende and biotite (Béland, 1967). The foliation of the gneisses and granites are gently dipping at an average angle of 20 to 30 degrees, and lithological units are generally parallel to them (Béland 1967). Field investigations and aerial photographic interpretations by Béland (1967) show that the pattern of the foliation is very sinuous with complex variations in the orientation. Béland (1967) said, "The final impression is that of plastically deformed gneisses, somewhat like a sheet of paper which is wrinkled and rumpled and not systematically folded along regularly arranged hinge lines."

The Sainte-Julienne Fault is located to the east of the Lanaudière region, where it is marked by a clearly visible escarpment oriented around 25°N and crosses the Saint-Julienne region (PACES LANAUDIÈRE 2019). Field investigations by Clark and Globensky (1976) followed the fault line of the Saint-Cuthbert Fault in the southeast direction of the Lanaudière region, particularly on outcrops observed at the following localities: Chicot, Bayonne, Rowboat, L'Assomption, along the crest of Joliette, and in many quarries. Southwest of Joliette, the Saint-Cuthbert Fault is located in the limestones of Trenton with an estimated longitudinal displacement of 131 m (Clark and Globensky 1976).

Data acquisition and processing

Outcrop data set

Field investigations for data collection was conducted during summer 2019 and summer 2020. Outcrops where fractures and other structural elements were not covered by mosses and lichens

were investigated. The sampling method used was the scanline technique, which consists of stretching a tape on an outcrop face and systematically sampling all fractures intersecting the tape from point A to B (Priest and Hudson 1981; Priest 2004; Chesnaux *et al.* 2009; Manda and Mabee 2010). For each intersected fracture in the scanline direction, fracture characteristics such as the dip, dip direction, aperture and persistence were recorded.

A total of 1421 fractures were sampled on 30 outcrops. These sampled fractures were unevenly distributed throughout the study area (Figure 1). The number of sampled fractures by outcrop varied between 8 and 349, while scanline lengths varied between 7 m and 235 m. The number of scanlines per outcrop varied according to the outcrop configuration. If the outcrop had more than one reachable outcrop face, the number of scanlines would be at least equal to the number of outcrop faces. The numbering system for outcrops on Figure 1 is related to the order of sampling.

Borehole geophysical survey

Boreholes were another source of fracture data, which provided insight on the fracture population and distribution in the subsurface. In this study, four boreholes (Figure 1) were investigated using acoustic and optical borehole imaging. The investigated depths were 43, 106, 79, and 28 m for boreholes SB5, SB6, RF1, and FE04, respectively. SB5 and FE04 had unstable and collapsing borehole walls which only allowed a partial investigation of the total borehole depth. All boreholes were unidirectional and vertical. A total number of 543 fractures were collected from RF1, SB5, FE04, and SB6, which respectively count for 206, 76, 96, and 165 fractures. In terms of fracture characteristics, the borehole imaging methods provided the dip, dip direction, and aperture of every encountered fracture.

Processing of structural data

Fracture sampling is, in itself, a biased activity, but necessary for engineering and geological studies as it provides essential information on the fracture network of the rock mass. Among the different

sources of biases, the geologists' own judgment during data collection (Andrews *et al.* 2019), the methods and approaches used to collect the data (Zeeb *et al.* 2013), and biases in the measurement of fracture parameters (Priest 1993; Jing and Stephansson 2007) can be also included. Depending on the sampling methods and fracture parameters, bias corrections have been proposed to attenuate their effect on analysis and interpretation of the data.

Given that the scanline sampling method and borehole imaging were used to collect fracture data for the present study, orientation biases existed and were reduced by applying a correction factor introduced by Terzaghi (1965). The orientation biases are related to the probability of sampling fractures, which is low for fracture with traces nearly parallel to the borehole or scanline direction (Terzaghi 1965; Priest 1993), while the sampling probability is high for fractures with traces almost perpendicular to the borehole or scanline direction (Terzaghi 1965; Priest 1993). Terzaghi (1965) proposed a geometrical correction factor, which considers the angle between the sampling line and the normal of the specific fracture. If we denote δ as the acute angle between the sampling line and the normal of a specific fracture, α_n/β_n as the trend/plunge of the fracture's normal vector, and α_s/β_s as the trend/plunge of the sampling line, the bias is reduced by assigning a weight w to the fracture (Priest 1993):

$$w = 1/\cos\delta \qquad \text{(Eq 1)}$$

where $$\cos\delta = |\cos(\alpha_n - \alpha_s)\cos\beta_n\cos\beta_s + \sin\beta_n\sin\beta_s| \qquad \text{(Eq 2)}$$

Further information on the correction of orientation biases is provided in Priest (1993) and Terzaghi (1965). As with the aforementioned orientation biases, the true spacing of a given fracture cluster (set) was different from the apparent spacing, particularly if fractures were not perfectly perpendicular to the sampling line (Priest 1993). If X_t and X_a denote the true and apparent spacing respectively, the true spacing is given by:

$$X_t = X_a\cos\delta \qquad \text{(Eq 3)}$$

Multiparametric similarity test

The different steps of the methodology are presented as a flowchart in Figure 2. The first step consisted of defining a cutoff threshold. Mahtab and Yegulalp (1984) defined cutoff threshold as a percentage of the sample size. Clusters that contain more fractures than the cutoff threshold are the main clusters of that sample. In this study, a cutoff threshold of 10% was used as proposed by Mahtab and Yegulalp (1984) and confirmed by the work of Kulatilake et al. (1990). Another important criterion that should be fulfilled by the clusters is linked to their dispersion parameter K (also called concentration factor or Fisher's constant) that should be greater than six (Mahtab and Yegulalp 1984). The parameter K assesses the concentration of the pole vectors around the mean pole vector of the cluster (Marcotte and Henry 2002). The smaller the K values the disperse the cluster (Mahtab *et al.* 1972; Priest 1993). The threshold of six ($K \geq 6$), defined by Mahtab and Yegulalp (1984), ensures the distribution of the pole vectors is in the neighborhood of the mean pole vector of the cluster. Details on the topic may be found in more specialized texts such as Mahtab *et al.* (1972) and Priest (1993). An estimate of the dispersion parameter K, of a cluster, is provided by Fisher (1953) as follows:

$$K = (N - 1)/(N - R) \qquad \text{(Eq 4)}$$

where N represents the total number of pole vectors in the fracture cluster and R is the resultant vector magnitude of the fracture cluster (resultant vector is also called mean vector). In our case, K values are computed using the program DIPS® (Rocsience Inc.). Hereafter, the term "cluster" designates "main cluster", as the multiparametric similarity test involved the use of main clusters only.

The second step consisted of performing the orientation similarity test between all clusters from adjacent samples. We considered I(i) and J(j) as the respective clusters from sample I and J. If $\alpha_{[I(i),J(j)]}$ represents the acute angle between the mean vectors of clusters I(i) and J(j), the sample I

and J are said to be similar with regard to their orientation, if Equation 5 is fulfilled. An illustration of the concept is provided in Figure 3.

$$\left|\cos \alpha_{[I(i),J(j)]}\right| > \cos \Psi_{I(i)} \, or \, \cos \Psi_{J(j)} \qquad \text{(Eq 5)}$$

where $\Psi_{I(i)}$ and $\Psi_{J(j)}$ are respectively the cones of confidence of the means of clusters I(i) and J(j). The cone of confidence provides the cone angle within which the true cluster mean lies, for a chosen degree of certainty (Mahtab and Yegulalp 1984). The degree of certainty is commonly selected between 90% and 99% (Priest 1993). In the present study, the chosen degree of certainty is of 95%. A more comprehensive discussion on the cone of confidence can be found in Priest (1993) and Mahtab *et al.* (1972).

The third step consisted of selecting only adjacent samples I and J that had similar clusters I(i) and J(j), with regard to their orientations, for further analysis in step 4. The fourth step examined the similarities of clusters I(i) and J(j) with respect to other fracture parameters. This examination was performed by using the hypothesis test and statistical analysis on clusters I(i) and J(j). The considered fracture parameters in the hypothesis testing were fracture spacing, aperture, and persistence. Clusters I(i) and J(j) were similar with regard to the enumerated fracture parameters, if they had the same distribution functions. However, fracture parameters such as spacing (Priest and Hudson 1976), aperture (Snow 1970) and persistence (Bonnet *et al.* 2001) tended to follow different distribution functions. Hence, in order to avoid an assumption about the distribution functions of clusters I(i) and J(j), nonparametric tests were performed. The most prominent feature of nonparametric tests is that no assumption is required on the underlying distribution functions of the fracture parameters for clusters I(i) and J(j) (Zimmerman 1987, 2011; Tanizaki 1997). The chosen nonparametric tests for the present study were the Mann-Whitney U (MW-U) test and the Kolmogorov-Smirnov (KS) test. The hypothesis tested by the two nonparametric tests was that the clusters I(i) and J(j), from the adjacent samples I and J, were from the same fracture population.

Thus, they had the same distribution for each fracture parameter. For readability purposes, details on the MW-U and KS tests are provided in Appendix I and Appendix II.

The fifth step consisted of selecting only adjacent samples I and J that had similar clusters I(i) and J(j), with regard to the chosen fracture parameters, for further analysis in step 6. The sixth step consisted of combining those adjacent samples I and J that had similar clusters. The seventh step consisted of repeating the combination process in step 6 for all the adjacent samples. The combination of samples led to the formation of groups of samples containing similar clusters. The eighth step consisted of examining whether each collected sample was within a group of samples. If yes, we proceeded to step 9, where samples in the same group were considered to be in the same structural domain. If no, the uncombined samples and the obtained groups were considered as a new set of samples and we repeated the process from step 2. The process was iterated until new combinations were no longer found.

Structural domain boundaries

The method described in the previous section did not allow the identification of boundaries between the different structural domains. The identification of structural domain boundaries mainly depends on the type of data. When structural domains are investigated along a borehole (Barnes *et al.* 1998), a tunnel (Zhan *et al.* 2020) or any other continuous rock exposure, the domain boundaries are relatively well defined. However, when domain boundaries are explored within a study site involving scattered fracture samples (Mahtab and Yegulalp 1984; Song *et al.* 2015), the location of domain boundaries become complex. The complexity is due to the lack of information between the samples and the fact that structural domain boundaries do not follow the geological unit boundaries (Mahtab and Yegulalp 1984; Vollmer 1990). It is therefore difficult to have unbiased and\or non-subjective domain boundaries.

In some cases, lineaments, which are linear features observable at the regional scale from satellite images or digital elevation models (DEMs), can be linked to major structural elements like faults

(Gleeson and Novakowski 2009). In such circumstances, the use of lineaments in the definition of the domain boundaries would be conceivable. However, in our case, the extraction of lineaments from a one-meter resolution LiDAR DEM brought out the main glacial erosion marks, which were judged unusable for the delimitation of the domain boundaries.

Voronoi diagrams (also called Thiessen polygons) are a non-subjective alternative in the delimitation of structural domain boundaries. Voronoi diagrams are used in several disciplines, including geography (Rhynsburger 1973) and hydrology (Fiedler 2003), to divide an area into **n** subareas, given **n** points (Aurenhammer 1991). The subdivision is done according to the nearest-neighbor rule, which affects each subarea to the nearest point (Aurenhammer 1991). Usually, polygons like subareas (see Figure 4) are created by computing perpendicular bisectors between all neighboring points (Brassel and Reif 1979). Further information on Voronoi diagrams can be found in Aurenhammer (1991). Voronoi diagrams also have the advantage of being implemented in GIS software such as QGIS (Beyhan *et al.* 2020) and ArcGIS (Dong 2008; Beyhan *et al.* 2020).

An application of the Voronoi diagram to the present study considered each fracture sample for the computation of the polygon-like subareas. Each sample was surrounded by a polygon that constituted the boundary between it and its adjacent samples (Figure 4 a, b). If two adjacent samples were similar, based on the methodology, the lines of the polygon that separated the two samples were removed (Figure 4 c). Conversely, if the samples were not similar, the line between the fracture samples remained as illustrated in Figure 4 c. In this example, samples d and e were considered from the same structural domain, while samples a, b, c and f were not similar to one another.

Structural domain determination

Orientation similarity test

To perform the similarity test, potentially similar fracture clusters of adjacent samples needed to be identified. Those potentially similar fracture clusters were clusters whose resultant vectors were visually almost parallel (at a low angle to each other) on the stereonet (figure 5). However, in order to be considered similar with regard to the orientation, they needed to fulfill the angular criteria provided in Equation 2. Figure 5 considers a subregion containing many fracture samples and plots the resultant vectors of all main fracture clusters on a stereonet; the poles of the resultants of potentially similar fracture clusters tend to form clusters as illustrated. If we denote I(i) and J(j), a pair of potential fracture clusters i and j (from samples I and J, respectively), one can compute the angle between I(i) and J(j), the cone of confidence of I(i) and J(j), and use Equation 5 to perform the orientation similarity test between the pair of fracture clusters.

For readability purposes, partial results of the orientation similarity test are presented in Table 1, while the complete table of the orientation similarity test, between all potential similar clusters, is presented in Appendix III. The results considered fracture clusters from 30 outcrops and four boreholes. The orientation similarity test was performed between fracture clusters of two adjacent outcrop samples, outcrop-borehole samples, or borehole samples. For each test, the similarity between the pair of potentially similar clusters was either rejected (R) or fail to be rejected (FTR).

At this stage, fracture samples that contained similar clusters could be grouped to form structural domains as a result of the orientation similarity test. However, many samples were not grouped given that the orientation similarity of several potentially similar clusters was rejected (see Table 1 and Appendix III). In Table 1 and Appendix III, outcrop samples are identified from numbers 1 to 30, while borehole samples are named SB5, SB6, FE04, and RF1. Comparing cluster **i** from sample **I** with cluster **j** from sample **J** is denoted **I(i)–J(j)**. Thus, **2(1)–3(1)** means comparing cluster 1 from sample 2 with cluster 1 from sample 3. Five groups of similar samples were formed, containing between two and ten fracture samples, whilst nine samples remained ungrouped (Figure 6). Similar samples were put in parentheses; the following groups were formed: M2 = (2, 20, 24, 25, and 26), M3 = (3, 27, SB6,

SB5), M6 = (6, FE04), M7 = (7, 23) and M8 = (8, 10, 11, 12, 13, 14, 15, 16, 17, and 30). Two of the groups showed orientation similarities between adjacent borehole samples and outcrop samples, which demonstrates the common practice in engineering geology of sampling fractures on outcrops for a better understanding of the subsurface fracture network.

Multiparametric similarity test

This section presents the results of the multiparametric similarity test, which further investigated the similarity of pairs of clusters with regard to the fracture parameters such as persistence, spacing, and aperture. For readability purposes, partial results of the multiparametric similarity test are presented in Table 2, while the complete table of the multiparametric similarity test between all clusters is provided in Appendix IV. In this study, the KS test and MW-U test were the two selected hypothesis tests used in the multiparametric similarity test, and only pairs of clusters which failed to be rejected in the orientation similarity test were considered. The level of significance α chosen for the KS test and the MW-U test was 0.05. Thus, a p-value that was greater than α indicated that the clusters were probably similar for the particular fracture parameter being tested. The overall similarity column, in Table 2 and Appendix IV, assesses the similarity between two clusters by taking into consideration the p-values of the two hypothesis tests for all the fracture parameters. Thus, the similarity between the two clusters was rejected, if either the KS test or the MW-U test rejected the similarity of the clusters for one parameter. The similarity between outcrop and borehole clusters was assessed without taking into consideration the persistence, as it could not be obtained from borehole data.

It is observed in Table 2 and Appendix IV that the KS test and the MW-U test provide generally analogous results. The similarity between clusters was either rejected for both tests or failed to be rejected. However, some exceptions occurred where the similarity was rejected by one test and failed to be rejected by the other. As the two tests behaved differently, if the similarity was rejected by the KS test while failing to be rejected by the MW-U test, this should indicate that the difference

between the two clusters' distribution functions was not of central tendency (i.e. not due to differences in means and medians). Conversely, if the similarity was rejected by the MW-U test while failing to be rejected by the KS test, the difference between the two distribution functions was most likely of central tendency nature. Li et al. (2014b), using a modified Miller's method, found comparable results between the KS test and the Wilcoxon rank sum test (equivalent to the MW-U test) in the assessment of the homogeneity between adjacent tunnel samples. In their results, the KS test rejected the homogeneity between samples that failed to be rejected by the Wilcoxon rank sum test, while the opposite did not occur. In the example illustrated in this paper, the similarity between clusters is accepted if it fails to be rejected by both hypothesis tests (KS-test and MW-U test). Although using two hypothesis tests increase the confidence of the similarity between clusters, as the result of one hypothesis test is verified by the other, the choice of using one or two hypothesis tests is left under the appreciation of the practitioner. It is a common practice in engineering geology to use one hypothesis test (Miller 1983; Song *et al.* 2015; Zhou *et al.* 2018) or two hypothesis tests (Li *et al.* 2014b; Zhang *et al.* 2016) in analysis of similarities between data sets. Arguably, choosing the right hypothesis test is much more important than the number of utilized hypothesis tests. Details on hypothesis tests are provided in more specialized books of statistics such as Johnson and Bhattacharyya (2010) and Alvo and Yu (2018).

In terms of fracture parameters, the rejection rate of the similarity between clusters was different from one parameter to the other. The rejection of the similarity between a pair of clusters, with regard to a given fracture parameter, indicated that they were most likely not similar. Thus, a pair of clusters could wrongly be considered similar if only one fracture parameter was considered. Similar rejection rates (from hypothesis tests analysis) for different fracture parameters were reported in studies by Zhang et al. (2016) and Zhou et al. (2019).

From the first iteration results (Table 2 and Appendix IV) of the multiparametric similarity test, three groups of similar samples G3, G13, and G20 were formed; these groups were constituted by samples

(3, 27, SB6), (13, 14, 15, 16, 17), and (20, 24, 26), respectively. A second iteration of the multiparametric similarity test was subsequently performed to integrate the ungrouped samples into the formed groups G3, G13, and G20. The overall similarity column presented in Table 3 shows that the overall similarities between adjacent ungrouped samples and the first iteration groups (G3, G13, and G20) were rejected. Under those circumstances, G3, G13, and G20 remained the same as in the first iteration; a spatial representation of the structural domains formed by those groups is illustrated in Figure 7.

The difference between Mahtab and Yegulalp's method (the orientation similarity test) and the multiparametric similarity test can be visually assessed by comparing Figure 6 and Figure 7. The groups of samples obtained from the multiparametric similarity test were shrunken groups of those obtained from the orientation similarity test, presented in the previous section. Thus, G3, G13, and G20 were the shrunken groups of the groups of samples M3, M8, and M2 respectively. Notably, two groups of samples (M6 and M7) that were similar according to Mahtab and Yegulalp's method were not similar with regard to the multiparametric similarity test. As the multiparametric similarity test takes into consideration other fracture parameters apart from just the fracture orientation, it was more capable of depicting discrepancies in the clusters' similarity. Hence, the multiparametric similarity test rejected the similarity of several adjacent samples that failed to be rejected through Mahtab and Yegulalp's method.

Fracture parameters combinations and structural domains

In the identification of fracture clusters, the reliability and benefit of adding other fracture parameters (infilling, aperture, persistence, roughness, hardness, and termination) to fracture orientation has been demonstrated in several studies (e.g., Liu et al., 2020; Tokhmechi et al., 2011). The practitioner should be aware of the biases that each fracture parameter is subjected to. These biases have an impact on the rejection rate of the similarity between clusters. Using multiple fracture parameters increases the reliability of the similarity between clusters but also adds up the

biases. Zhou et al. (2019) employed a modified Miller's method, which includes fracture orientation, persistence, and aperture and performed an experiment with simulated fracture data and real fracture data. The experiment consisted of identifying similar samples in both data sets. Zhou et al. (2019) did not find pairs of similar samples in the real fracture data, while they found similar samples in the simulated fracture data. In general, the more parameters we use the less likely that pairs of similar samples would be identified in complex natural fracture systems.

Information from Table 2 and Table 3 revealed that different fracture parameter combinations would lead to different results of similar sample groups. Figure 8 illustrates the effect of different combinations of fracture parameters on the grouping of fracture samples into structural domains by performing the multiparametric similarity test with two combinations of fracture parameters. The first combination (illustrated with red circles in Figure 8) considered fracture orientation and spacing, while the second combination (illustrated with black circles) considered all the parameters (fracture orientation, trace length, spacing, and aperture). In practice, choosing the fracture parameters combination to be used in the multiparametric similarity test should be dictated by the project objectives. For hydrogeological studies, the hydraulic conductivity in fractured rocks is mainly influenced by the fracture orientation, persistence, spacing, and aperture (Scesi and Gattinoni 2010; Wenli *et al.* 2019). Thus, it is necessary to consider all these fracture parameters in the multiparametric similarity test for studies of fluid circulation in the rock mass. For geotechnical, mining, and engineering geology studies, several "rock quality" indexes and parameters are used to assess the physical properties of rocks such as the Rock Quality Design (RQD) and the rock mass quality Q (Barton *et al.* 1974; Schön 2015). The RQD and Q assess the rock mass strength. For a project investigating the rock mass strength, the present method should be modified accordingly, to take into consideration the relevant parameters.

In a study area with complex fracture networks, using many fracture parameters in the multiparametric similarity test may lead to a "lack of domaining". The lack of domaining is the lack of

finding similar samples. Depending on the practitioner, the lack of domaining can be problematic, but others would see it as evidence of complex fracture networks. For instance, in hydrogeological studies, the lack of domaining can help explain why adjacent boreholes in crystalline aquifers can yield very different exploitation discharges and rock mass permeabilities. The issue of borehole yield in crystalline rocks is well known to hydrogeologists and several researchers (Bridge Moore *et al.* 2002; Banks *et al.* 2010; Holland and Witthüser 2011; Roques *et al.* 2016) have investigated factors that are related to borehole yield in crystalline aquifers; however, the results are far from being generalizable. If one is confronted with a lack of domaining in complex fracture networks and still want to achieve many similar samples, the practitioner can reduce the number of fracture parameters or choose a lower α value in the hypothesis test. It should be noted that the method (Figure 2) proposed in this paper is flexible enough to allow the practitioner to choose the hypothesis test (step 4 of the multiparametric similarity test) that is well suited to the research objectives and the data collected.

Voronoi diagrams could be used for the delimitation of structural domain boundaries. Figure 9 illustrates the use of Voronoi diagrams in the delimitation of structural domain boundaries by considering fracture orientation, persistence, spacing, and aperture. Similar maps could be produced for each combination of fracture parameters. The resulting compartmentalization (Figure 9) subdivided the study area into 24 compartments of homogeneous fracture networks. Therefore, each compartment could be characterized by the properties of its fracture network such as the number of fracture clusters and the fracture cluster parameters (e.g., fracture orientation, persistence, aperture, and spacing). A summary of each compartment's fracture characteristics is provided in Appendix V. The compartmentalization was particularly useful in regional studies as it considered the heterogeneity and complexity of the existing fracture networks in the study area. For hydrogeological studies, knowing the fracture clusters and fracture characteristics allows the assessment of both the hydraulic conductivity and the anisotropy of the hydraulic conductivity, as

exemplified by DesRoches et al. (2014). Thus, for each structural domain (compartment), the hydraulic properties of the rock mass could be estimated.

Conclusion

Fracture samples comprise many fractures, which are described by several fracture parameters. Among the most important fracture parameters for fluid circulation are fracture orientation, aperture, persistence, and spacing. In this study we developed a cluster-based method to group and delineate fracture samples into structural domains in a rock mass. The method improved the similarity test proposed by Mahtab and Yegulalp (1984) by adding the fracture parameters, such as spacing, persistence, and aperture to the original method, which used only fracture orientation. The multiparametric similarity test is more reliable as it adds a degree of certainty to the similarity of samples by testing their similarity on multiple fracture parameters. Consequently, it provides higher confidence in the delineation of structural domains, which in return implies a better characterization of fracture networks in a study area.

The assessment of the similarity between two adjacent samples is made via clusters of samples. Ultimately, adjacent samples are similar if they share clusters that are similar with regard to their orientation, spacing, persistence, and aperture. Two clusters from adjacent samples are similar with regard to their orientation if their resultant vectors have the same orientation according to a defined criterion. The similarity between the two clusters with regard to their spacing, persistence, and aperture is assessed by means of nonparametric hypothesis testing, such as the KS test and the MW-U test.

The multiparametric similarity test has been applied to a data set comprising 30 outcrop samples and four borehole samples. The results showed that the KS test and the MW-U test perform almost equally in the identification of similar samples. Performing the multiparametric similarity test with different combinations of fracture parameters leads to different groups of similar samples. In general, the more parameters used in the multiparametric similarity test, the fewer similar samples

will be identified. This highlights that, when using only one parameter such as fracture orientation, it is possible to mistakenly consider two adjacent samples similar, while in reality they are dissimilar with regard to spacing or persistence or aperture. However, the practitioner should be conscious of the biases of fracture parameters. It is advisable that corrections are applied to reduce the fracture parameter biases, which is discussed in detail in the studies by Chilès and Marsily (1993), Priest (1993), and Jing and Stephansson (2007).

To remove subjectivity in the delineation of domain boundaries, we also proposed using the Voronoi diagram, which divides the study area into a number of subareas corresponding to the number of samples. Each fracture sample is assigned a subarea. If two adjacent samples are similar, the boundary between the two is removed and retained if the two samples are dissimilar. In general, the more fracture samples we have, the more accurate the domain boundaries.

The multiparametric similarity test has the potential to be used in all studies involving a thorough analysis of fluid circulation in the rock mass and other geomechanical studies (e.g., tunneling, and dam construction). As the method exclusively uses fracture parameters to determine the structural domains, the underlying hypothesis of the method is that the hydromechanical properties of the rock mass are homogenous in the same fracture network, hence in the same structural domain. While this hypothesis is commonly accepted and theoretically sound, further studies are required to investigate the homogeneity of the hydromechanical properties of the rock mass within the structural domains. In this context, the practice of delimiting the structural domains of a study area would be an iterative process where the practitioner finds the right fracture combination that leads to structural domains of homogeneous hydraulic (e.g., hydraulic conductivity) and/or mechanical (e.g., RQD) properties.

Appendices

Appendix A: Mann-Whitney U test

The Mann-Whitney U test (MW-U test) is generally considered to be the nonparametric equivalent of the parametric t-test, as both tests are used for identifying discrepancies in central tendency between two samples (Hart 2001; Feltovich 2003; Krzywinski and Altman 2014). However, in terms of statistical power, Zimmerman (2011) found the MW-U test to be considerably more powerful than the t-test (a power difference of 0.1 to 0.3) when the samples' distributions were skewed, such as lognormal and exponential. Conversely, a power difference of 0.01 to 0.04 in favor of the t-test for symmetric distributions like the uniform and normal was reported (Zimmerman 2011). The statistical power is the probability to correctly reject the null hypothesis (H_0) when it is false (Feltovich 2003; Kolassa 2020). In this study, the null hypothesis is that the two clusters from the adjacent samples are from the same fracture population. Thus, they have the same distribution for each fracture parameter.

Let us reconsider clusters I(i) and J(j), from samples I and J, containing respectively n and m number of fractures; let X_1, …, X_n and Y_1, …, Y_m be the two independent fracture clusters comprising I(i) and J(j), respectively. The first step in the MW-U test consists of combining and arranging, from least to greatest, the two clusters (I(i) and J(j)) into a cluster of size N = n+m. Let us denote R (Y_a), the rank of Y_a in the combined cluster and S (Y_a) be the rank of Y_a among the elements Y_1, …, Y_m. Then the MW-U statistic can be defined as (Alvo and Yu 2018):

$$U(X,Y) = \sum_{a=1}^{m} R(Y_a) - \sum_{a=1}^{m} S(Y_a) = W - \frac{m(m+1)}{2} \qquad (Eq\ A.1)$$

where $W = \sum_{a=1}^{m} R(Y_a)$ represents the Wilcoxon statistics. It should be noted that for large fracture clusters (n and m > 20 (Siegel 1956)), the distribution of U (X, Y) quickly approaches the normal distribution (Siegel 1956; Alvo and Yu 2018). With a mean and variance (var) of:

$$mean = \mu_U = \frac{nm}{2} \qquad (Eq\ A.2)$$

$$Var = \frac{nm(N+1)}{12} \qquad (Eq\ A.3)$$

Therefore, to determine an estimate of the level of significance of an observed value U (p-value):

$$z = \frac{U - \mu_U}{\sqrt{var}} = \frac{U - \frac{nm}{2}}{\sqrt{\frac{nm(N+1)}{12}}} \qquad (Eq\ A.4)$$

The two-tailed p-value is then given by:

$$p - value = 2P\left(z \leq \frac{U - \frac{nm}{2}}{\sqrt{\frac{nm(N+1)}{12}}}\right) \qquad (Eq\ A.5)$$

As the MW-U test is based on ranks, corrections for eventual ties in the ranking process are required when they occur (Siegel 1956; Alvo and Yu 2018). In this case, changes occur in the variance equation (Eq A.2), while the mean does not change (Eq A.3). Thus, the equation for the estimate of the p-value (Eq A.5) will change accordingly. The new variance which corrects for ties is given by Alvo and Yu (2018) as:

$$Var_{ties} = \frac{nm(N+1)}{12} - \frac{nm\left(\sum_{i=1}^{k} d_i^3 - d_i\right)}{12N(N-1)} \qquad (Eq\ A.6)$$

where k represents the number of tied groups if we consider that observations with the same rank form a group of observation, while d_i is the number of observations tied in the i^{th} tied group (i =1, 2, …, k).

By using the normal approximation, an estimate of the p-value may lead to inaccurate results (Mehta and Patel 2011). A more accurate method of obtaining the p-value is the exact test, which provides the exact p-value (Mehta and Patel 2011; Alvo and Yu 2018). The exact test uses a resampling method, involving the permutation of the observed data (within a cluster), in all possible ways, so that a histogram of test statistic values (U value of each possible outcome) that estimates the null distribution can be created (Alvo and Yu 2018). The interested reader is directed to a more specialized book such as the one by Alvo and Yu, (2018). One downside of the exact test is that it is

computationally intensive as, in the permutation process, all possible outcomes need to be computed (Mehta and Patel 2011; Alvo and Yu 2018). Therefore, in case of large data, the Monte Carlo method provides a good alternative as it does not compute all possible outcomes (Mehta and Patel 2011). In this research, all the reported p-values are obtained via the exact test or the Monte Carlo method. The used level of significance α, below which the null hypothesis is rejected, is 0.05.

Appendix B – Kolmogorov-Simonov test

Unlike the MW-U test, the two-tailed Kolmogorov-Smirnov test (KS test) is a more general test which is responsive to any kind of differences between the distribution functions of the two independent samples (Siegel 1956; Wilcox 1997; Bonnini *et al.* 2014). The differences are evaluated on the basis of the maximum vertical difference between the two empirical distribution functions (Siegel 1956). Thus, if the distribution functions have a large distance between each other at any point, in comparison to a critical distance of the KS distribution for a given level of significant α, it indicates that the samples may come from different populations (Siegel 1956). In terms of statistical power, the KS test is reported to have a minor advantage over the MW-U test for small samples, while the MW-U test has a minor advantage over the KS test for large samples (Siegel 1956).

Let X_1, …, X_n and Y_1, …, Y_m be the two independent fracture clusters composing I(i) and J(j), respectively. Let us consider $F_n(x)$ and $F_m(x)$ the respective cumulative empirical distribution function of X_1, …, X_n and Y_1, …, Y_m, such as

$$\begin{cases} F_n(x) = \dfrac{number\ of\ samples\ X's \leq x}{n} \\ F_m(x) = \dfrac{number\ of\ samples\ Y's \leq x}{m} \end{cases} \qquad (Eq\ B.1)$$

The KS test concentrates on the largest observed departure between $F_n(x)$ and $F_m(x)$ and is formulated as (Siegel 1956; Wilcox 1997):

$$D = maximum|F_n(x) - F_m(x)| \qquad (Eq\ B.2)$$

where D is the Kolmogorov-Smirnov distance function. A good estimate of the p-value is provided by the exact test, which is described in the previous section. In this research, all the reported Kolmogorov-Smirnov two-tailed test p-values are estimated by means of the exact test. Given that the chosen level of significance α is 0.05 and the null hypothesis is that the two samples belong to the same population, the null hypothesis is rejected for all p-values that are below 0.05.

Appendix C – Results of the orientation similarity tests between clusters

The results of the orientation similarity tests between clusters I(i) and J(j), respectively, from adjacent samples I and J are shown in the table below. R and FTR stand for rejected and failed to be rejected, respectively.

Appendix D – Results of the first iteration multiparametric similarity test

The results of the first iteration multiparametric similarity test, using fracture orientation, persistence, spacing and aperture parameters is shown in the table below. KS test and MW-U test refer to the Kolmogorov-Smirnov test and the Mann-Whitney U test. R and FTR stand for rejected and failed to be rejected, respectively. P-values in bold are higher than 0.05.

Appendix E –Fracture clusters and fracture characteristics of structural domains.

The fracture clusters and fracture characteristics of structural domains obtained by the multiparametric similarity test using fracture orientation, persistence, spacing, and aperture parameter. The characteristics of structural domains correspond to the compartmentalization illustrated in Figure 9.

Acknowledgements

The authors would like to thank the team of the project “Programme d’acquisition de connaissances sur les eaux souterraines du Québec (PACES)”, from the Université du Québec à Chicoutimi, who helped with data collection.

Author contributions

Attoumane Abi: Conceptualization, Methodology, Software, Validation, Writing original draft, Writing - review & editing. Julien Walter: Conceptualization, Supervision, Writing - review & editing. Ali Saeidi: Supervision, Writing - review & editing. Romain Chesnaux: Supervision, Writing - review & editing.

Funding

This project was funded by the Programme d'acquisition de connaissances sur les eaux souterraines du Québec (PACES), with contributions from the Ministère de l'Environnement et de la Lutte contre les Changements Climatiques (MELCC) du Québec, The Université du Québec à Chicoutimi (UQAC), and the four county municipalities of the Lanaudière region (Autray, Matawinie, Montcalm, Assomption).

Data availability

The raw data is available and accessible through the authors.

References

Alvo, M. and Yu, P. 2018. *A Parametric Approach to Nonparametric Statistics*. Springer Series in the Data Sciences, https://doi.org/10.1007/978-3-319-94153-0.

Andrews, B.J., Roberts, J.J., Shipton, Z.K., Bigi, S., Tartarello, M.C. and Johnson, G. 2019. How do we see fractures? Quantifying subjective bias in fracture data collection. *Solid Earth*, **10**, 487–516, https://doi.org/10.5194/se-10-487-2019.

Aurenhammer, F. 1991. Voronoi diagrams—a survey of a fundamental geometric data structure. *ACM Computing Surveys*, **23**, 345–405, https://doi.org/10.1145/116873.116880.

Banks, D., Gundersen, P., Gustafson, G., Mäkelä, J. and Morland, G. 2010. Regional similarities in the distributions of well yield from crystalline rocks in Fennoscandia. *Norges Geologiske Undersokelse Bulletin*, **450**, 33–47.

Barnes, R.P., Dee, S.J., Sanderson, D.J. and Bowden, R.A. 1998. Interpretation of structural domains in discontinuity data from Nirex deep boreholes at Sellafield. *Proceedings of the Yorkshire Geological Society*, **52**, 177–187, https://doi.org/10.1144/pygs.52.2.177.

Barton, N., Lien, R. and Lunde, J. 1974. Engineering classification of rock masses for the design of tunnel support. *Rock mechanics*, **6**, 189–236, https://doi.org/10.1007/BF01239496.

Béland, R. 1967. *Région de Saint-Gabriel-de-Brandon, Comtes de Joliette, Berthier et Maskinongé*. Geological reports **RG 133**.

Beyhan, B., Güler, C. and Tağa, H. 2020. An algorithm for maximum inscribed circle based on Voronoi diagrams and geometrical properties. *Journal of Geographical Systems*, **22**, 391–418, https://doi.org/10.1007/s10109-020-00325-3.

Bonnet, E., Bour, O., Odling, N.E., Davy, P., Main, I., Cowie, P. and Berkowitz, B. 2001. Scaling of fracture systems in geological media. *Reviews of Geophysics*, **39**, 347–383, https://doi.org/10.1029/1999RG000074.

Bonnini, S., Corain, L., Marozzi, M. and Salmaso, L. 2014. *Nonparametric Hypothesis Testing: Rank and Permutation Methods with Applications in R*, $ {nombre}er édition.

Brassel, K.E. and Reif, D. 1979. A Procedure to Generate Thiessen Polygons. *Geographical Analysis*, **11**, 289–303, https://doi.org/10.1111/j.1538-4632.1979.tb00695.x.

Bridge Moore, R., E Schwarz, G., F Clark, S., Walsh, G. and Degnan, J. 2002. Factors Related to Well Yield in the Fractured-Bedrock Aquifer of New Hampshire. *US Geological Survey Professional Paper*.

Chesnaux, R., Allen, D.M. and Jenni, S. 2009. Regional fracture network permeability using outcrop scale measurements. *Engineering Geology*, **108**, 259–271, https://doi.org/10.1016/j.enggeo.2009.06.024.

Chilès, J.-P. and Marsily, G. de. 1993. 4 - Stochastic Models of Fracture Systems and Their Use in Flow and Transport Modeling. *In*: Bear, J., Tsang, C.-F. and de Marsily, G. (eds) *Flow and Contaminant Transport in Fractured Rock*. 169–236., https://doi.org/10.1016/B978-0-12-083980-3.50008-5.

Clark, T.H. and Globensky, Y. 1976. *Région de Sorel et partie sud-est de Saint-Gabriel-de-Brandon*. Geological reports **RG 155**.

DesRoches, A., Danielescu, S. and Butler, K. 2014. Structural controls on groundwater flow in a fractured bedrock aquifer underlying an agricultural region of northwestern New Brunswick, Canada. *Hydrogeology Journal*, **22**, 1067–1086, https://doi.org/10.1007/s10040-014-1134-0.

Dong, P. 2008. Generating and updating multiplicatively weighted Voronoi diagrams for point, line and polygon features in GIS. *Computers & Geosciences*, **34**, 411–421, https://doi.org/10.1016/j.cageo.2007.04.005.

Feltovich, N. 2003. Nonparametric Tests of Differences in Medians: Comparison of the Wilcoxon–Mann–Whitney and Robust Rank-Order Tests. *Experimental Economics*, **6**, 273–297, https://doi.org/10.1023/A:1026273319211.

Fiedler, F.R. 2003. Simple, Practical Method for Determining Station Weights Using Thiessen Polygons and Isohyetal Maps. *Journal of Hydrologic Engineering*, **8**, 219–221, https://doi.org/10.1061/(ASCE)1084-0699(2003)8:4(219).

Fisher, R.A. 1953. Dispersion on a sphere. *Proceedings of the Royal Society of London. Series A. Mathematical and Physical Sciences*, **217**, 295–305, https://doi.org/10.1098/rspa.1953.0064.

Gleeson, T. and Novakowski, K. 2009. Identifying watershed-scale barriers to groundwater flow: Lineaments in the Canadian Shield. *GSA Bulletin*, **121**, 333–347, https://doi.org/10.1130/B26241.1.

Guo, L., Wu, L., Zhang, J., Liao, M. and Ji, Y. 2020. Identification of homogeneous region boundaries of fractured rock masses in candidate sites for Chinese HLW repository. *Bulletin of Engineering Geology and the Environment*, **79**, 4221–4243, https://doi.org/10.1007/s10064-020-01837-4.

Hamm, S.-Y., Kim, M., Cheong, J.-Y., Kim, J.-Y., Son, M. and Kim, T.-W. 2007. Relationship between hydraulic conductivity and fracture properties estimated from packer tests and borehole data in a fractured granite. *Engineering Geology*, **92**, 73–87, https://doi.org/10.1016/j.enggeo.2007.03.010.

Hart, A. 2001. Mann-Whitney test is not just a test of medians: differences in spread can be important. *BMJ*, **323**, 391–393, https://doi.org/10.1136/bmj.323.7309.391.

Holland, M. and Witthüser, K.T. 2011. Evaluation of geologic and geomorphologic influences on borehole productivity in crystalline bedrock aquifers of Limpopo Province, South Africa. *Hydrogeology Journal*, **19**, 1065–1083, https://doi.org/10.1007/s10040-011-0730-5.

Jing, L. and Stephansson, O. 2007. 5 - The Basics of Fracture System Characterization – Field Mapping and Stochastic Simulations. *In*: Jing, L. and Stephansson, O. (eds) *Developments in Geotechnical Engineering*. 147–177., https://doi.org/10.1016/S0165-1250(07)85005-X.

Johnson, R.A. and Bhattacharyya, G.K. 2010. *Statistics - Principles and Methods*, 6th ed.

Kolassa, J.E. 2020. *An Introduction to Nonparametric Statistics*, 1st edition.

Krzywinski, M. and Altman, N. 2014. Nonparametric tests. *Nature Methods*, **11**, 467–468, https://doi.org/10.1038/nmeth.2937.

Kulatilake, P.H.S.W., Wathugala, D.N., Poulton, M. and Stephansson, O. 1990. Analysis of structural homogeneity of rock masses. *Engineering Geology*, **29**, 195–211, https://doi.org/10.1016/0013-7952(90)90050-B.

Kulatilake, P.H.S.W., Fiedler, R. and Panda, B.B. 1997. Box fractal dimension as a measure of statistical homogeneity of jointed rock masses. *Engineering Geology*, **48**, 217–229, https://doi.org/10.1016/S0013-7952(97)00045-8.

Li, Y., Wang, Q., Chen, J., Han, L., Zhang, W. and Ruan, Y. 2014a. Determination of structural domain boundaries in jointed rock masses: An example from the Songta dam site, China. *Journal of Structural Geology*, **69**, 179–188, https://doi.org/10.1016/j.jsg.2014.10.011.

Li, Y., Wang, Q., Chen, J., Han, L. and Song, S. 2014b. Identification of structural domain boundaries at the Songta dam site based on nonparametric tests. *International Journal of Rock Mechanics and Mining Sciences*, **70**, 177–184, https://doi.org/10.1016/j.ijrmms.2014.04.018.

Li, Y., Wang, Q., Chen, J., Song, S., Ruan, Y. and Zhang, Q. 2015. A Multivariate Technique for Evaluating the Statistical Homogeneity of Jointed Rock Masses. *Rock Mechanics and Rock Engineering*, **48**, 1821–1831, https://doi.org/10.1007/s00603-014-0678-6.

Liu, T., Zheng, J. and Deng, J. 2020. A new iteration clustering method for rock discontinuity sets considering discontinuity trace lengths and orientations. *Bulletin of Engineering Geology and the Environment*, https://doi.org/10.1007/s10064-020-01921-9.

Mahtab, M.A. and Yegulalp, T.M. 1984. Similarity Test For Grouping Orientation Data In Rock Mechanics. *In*: The 25th U.S. Symposium on Rock Mechanics (USRMS).

Mahtab, M.A., Bolstad, D.D., Alldredge, J.R. and Shanley, R.J. 1972. *Analysis of Fracture Orientations for Input to Structural Models of Discontinuous Rock*.

Manda, A.K. and Mabee, S.B. 2010. Comparison of three fracture sampling methods for layered rocks. *International Journal of Rock Mechanics and Mining Sciences*, **47**, 218–226, https://doi.org/10.1016/j.ijrmms.2009.12.004.

Marcotte, D. and Henry, E. 2002. Automatic joint set clustering using a mixture of bivariate normal distributions. *International Journal of Rock Mechanics and Mining Sciences*, **39**, 323–334, https://doi.org/10.1016/S1365-1609(02)00033-3.

Martin, M.W. and Tannant, D.D. 2004. A technique for identifying structural domain boundaries at the EKATI Diamond Mine. *Engineering Geology*, **74**, 247–264, https://doi.org/10.1016/j.enggeo.2004.04.001.

Mehta, C.R. and Patel, N.R. 2011. *IBM SPSS Exact Tests*.

Miller, S.M. 1983. A statistical method to evaluate homogeneity of structural populations. *Journal of the International Association for Mathematical Geology*, **15**, 317–328, https://doi.org/10.1007/BF01036073.

PACES LANAUDIÈRE. 2019. *Rapport D'étape De La Phase I Basée Sur Les Données Existantes Et Planification Révisée De La Phase II*. **I**PACES LANAUDIÈRE.

Phi, T.T. 2016. Some Results of Quantitative Analysis of Fracture Orientation Distribution along the Segment Tien Yen-Mui Chua of Cao Bang-Tien Yen Fault Zone, Quang Ninh Province, Viet Nam. *Journal of Geological Resource and Engineering*, **2**, 81–88, https://doi.org/10.17265/2328-2193/2016.02.004.

Priest, S.D. 1993. *Discontinuity Analysis for Rock Engineering*, https://doi.org/10.1007/978-94-011-1498-1.

Priest, S.D. 2004. Determination of Discontinuity Size Distributions from Scanline Data. *Rock Mechanics and Rock Engineering*, **37**, 347–368, https://doi.org/10.1007/s00603-004-0035-2.

Priest, S.D. and Hudson, J.A. 1976. Discontinuity spacings in rock. *International Journal of Rock Mechanics and Mining Sciences & Geomechanics Abstracts*, **13**, 135–148, https://doi.org/10.1016/0148-9062(76)90818-4.

Priest, S.D. and Hudson, J.A. 1981. Estimation of discontinuity spacing and trace length using scanline surveys. *International Journal of Rock Mechanics and Mining Sciences & Geomechanics Abstracts*, **18**, 183–197, https://doi.org/10.1016/0148-9062(81)90973-6.

QuocPhi, N., SangGi, H., TruongThanh, P. and Phuong, N. 2012. Structural Domain Identification by Fracture Orientation and Fracture Density in Rock Mass | IJG:International Journal of Geoinformatics. *International Journal of Geoinformatics*, **8**, 35–40.

Rhynsburger, D. 1973. Analytic Delineation of Thiessen Polygons*. *Geographical Analysis*, **5**, 133–144, https://doi.org/10.1111/j.1538-4632.1973.tb01003.x.

Rivers, T., Martignole, J., Gower, C.F. and Davidson, A. 1989. New tectonic divisions of the Grenville Province, Southeast Canadian Shield. *Tectonics*, **8**, 63–84, https://doi.org/10.1029/TC008i001p00063.

Roques, C., Bour, O., et al. 2014. Hydrological behavior of a deep sub-vertical fault in crystalline basement and relationships with surrounding reservoirs. *Journal of Hydrology*, **509**, 42–54, https://doi.org/10.1016/j.jhydrol.2013.11.023.

Roques, C., Bour, O., Aquilina, L. and Dewandel, B. 2016. High-yielding aquifers in crystalline basement: insights about the role of fault zones, exemplified by Armorican Massif, France. *Hydrogeology Journal*, **24**, 2157–2170, https://doi.org/10.1007/s10040-016-1451-6.

Scesi, L. and Gattinoni, P. 2010. *Water Circulation in Rocks*.

Scesi, L. and Gattinoni, P. 2012. Methods and models to determine the groundwater flow in rock masses: Review and examples. *Environmental Science, Engineering and Technology*, 1–54.

Schön, J.H. 2015. Geomechanical Properties. *In*: *Developments in Petroleum Science*. 269–300., https://doi.org/10.1016/B978-0-08-100404-3.00007-X.

Siegel, S. 1956. *Nonparametric Statistics for the Behavioral Sciences*.

Singhal, B.B.S. and Gupta, R.P. 2010. *Applied Hydrogeology of Fractured Rocks: Second Edition*, 2nd ed.

Snow, D.T. 1970. The frequency and apertures of fractures in rock. *International Journal of Rock Mechanics and Mining Sciences & Geomechanics Abstracts*, **7**, 23–40, https://doi.org/10.1016/0148-9062(70)90025-2.

Song, S., Wang, Q., Chen, J., Cao, C., Li, Y. and Zhou, X. 2015. Demarcation of homogeneous structural domains within a rock mass based on joint orientation and trace length. *Journal of Structural Geology*, **80**, 16–24, https://doi.org/10.1016/j.jsg.2015.08.006.

Song, S., Sun, F., et al. 2018. Identification of structural domains by considering multiple discontinuity characteristics: a case study of the Songta Dam. *Bulletin of Engineering Geology and the Environment*, **77**, 1589–1598, https://doi.org/10.1007/s10064-017-1024-5.

Tanizaki, H. 1997. Power comparison of non-parametric tests: Small-sample properties from Monte Carlo experiments. *Journal of Applied Statistics*, **24**, 603–632, https://doi.org/10.1080/02664769723576.

Terzaghi, R.D. 1965. Sources of Error in Joint Surveys. *Géotechnique*, **15**, 287–304, https://doi.org/10.1680/geot.1965.15.3.287.

Tokhmechi, B., Memarian, H., Moshiri, B., Rasouli, V. and Noubari, H.A. 2011. Investigating the validity of conventional joint set clustering methods. *Engineering Geology*, **118**, 75–81, https://doi.org/10.1016/j.enggeo.2011.01.002.

Turner, F.J., Turner, F.J. and Weiss, L.E. 1963. *Structural Analysis of Metamorphic Tectonites*.

Vollmer, F.W. 1990. An application of eigenvalue methods to structural domain analysis. *GSA Bulletin*, **102**, 786–791, https://doi.org/10.1130/0016-7606(1990)102<0786:AAOEMT>2.3.CO;2.

Wenli, Y., Sharifzadeh, M., Yang, Z., Xu, G. and Fang, Z. 2019. Assessment of fracture characteristics controlling fluid flow in discrete fracture networks (DFN). *Journal of Petroleum Science and Engineering*, https://doi.org/10.1016/j.petrol.2019.04.011.

Wilcox, R.R. 1997. Some practical reasons for reconsidering the Kolmogorov-Smirnov test. *British Journal of Mathematical and Statistical Psychology*, **50**, 9–20, https://doi.org/10.1111/j.2044-8317.1997.tb01098.x.

Zeeb, C., Gomez-Rivas, E., Bons, P.D., Virgo, S. and Blum, P. 2013. Fracture network evaluation program (FraNEP): A software for analyzing 2D fracture trace-line maps. *Computers & Geosciences*, **60**, 11–22, https://doi.org/10.1016/j.cageo.2013.04.027.

Zhan, J., Pang, Y., Chen, J., Cao, C., Song, S. and Zhou, X. 2020. A Progressive Framework for Delineating Homogeneous Domains in Complicated Fractured Rock Masses: A Case Study from the Xulong Dam Site, China. *Rock Mechanics and Rock Engineering*, **53**, 1623–1646, https://doi.org/10.1007/s00603-019-01999-y.

Zhang, W., Zhao, Q., Huang, R., Chen, J., Xue, Y. and Xu, P. 2016. Identification of structural domains considering the size effect of rock mass discontinuities: A case study of an underground excavation in Baihetan Dam, China. *Tunnelling and Underground Space Technology*, **51**, 75–83, https://doi.org/10.1016/j.tust.2015.10.026.

Zhou, W. and Maerz, N.H. 2002. Implementation of multivariate clustering methods for characterizing discontinuities data from scanlines and oriented boreholes. *Computers & Geosciences*, **28**, 827–839, https://doi.org/10.1016/S0098-3004(01)00111-X.

Zhou, X., Chen, J., Ruan, Y., Zhang, W., Song, S. and Zhan, J. 2018. Demarcation of Structural Domains in Fractured Rock Masses Using a Three-Parameter Simultaneous Analysis Method. *Advances in Civil Engineering*, **2018**, e9358098, https://doi.org/10.1155/2018/9358098.

Zhou, X., Chen, J., Zhan, J., Song, S. and Cao, C. 2019. Identification of structural domains considering the combined effect of multiple joint characteristics. *Quarterly Journal of Engineering Geology and Hydrogeology*, **52**, 375–385, https://doi.org/10.1144/qjegh2018-091.

Zhu, J. 2019. Effective hydraulic conductivity of discrete fracture network with aperture-length correlation. *Geosciences Journal*, https://doi.org/10.1007/s12303-019-0025-8.

Zimmerman, D.W. 1987. Comparative Power of Student T Test and Mann-Whitney U Test for Unequal Sample Sizes and Variances. *The Journal of Experimental Education*, **55**, 171–174, https://doi.org/10.1080/00220973.1987.10806451.

Zimmerman, D.W. 2011. A simple and effective decision rule for choosing a significance test to protect against non-normality. *British Journal of Mathematical and Statistical Psychology*, **64**, 388–409, https://doi.org/10.1348/000711010X524739.

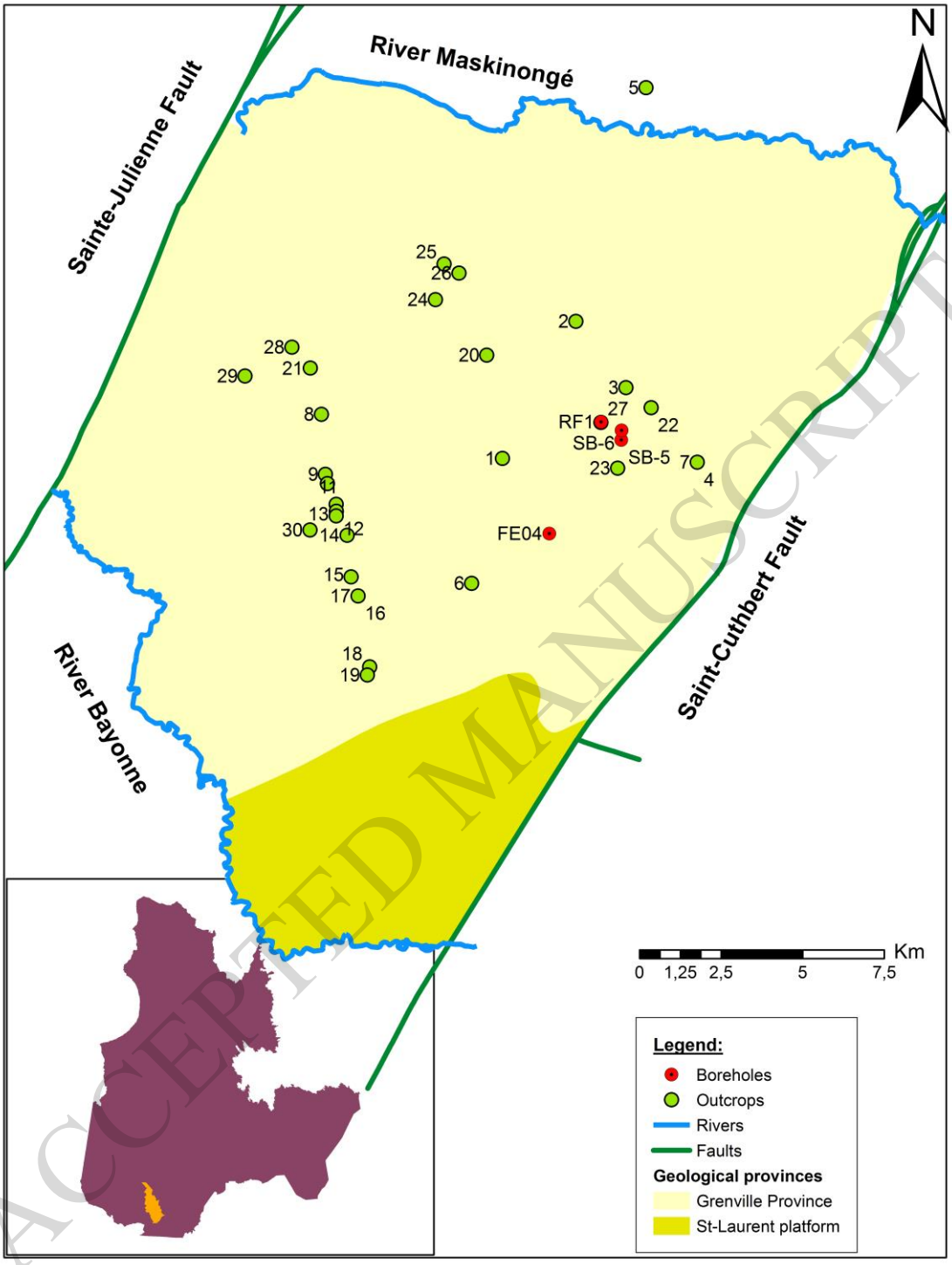

Figure 1: Illustration of the geological formations in the study area along with the spatial distribution of the sampling points within the study area, the type of data.

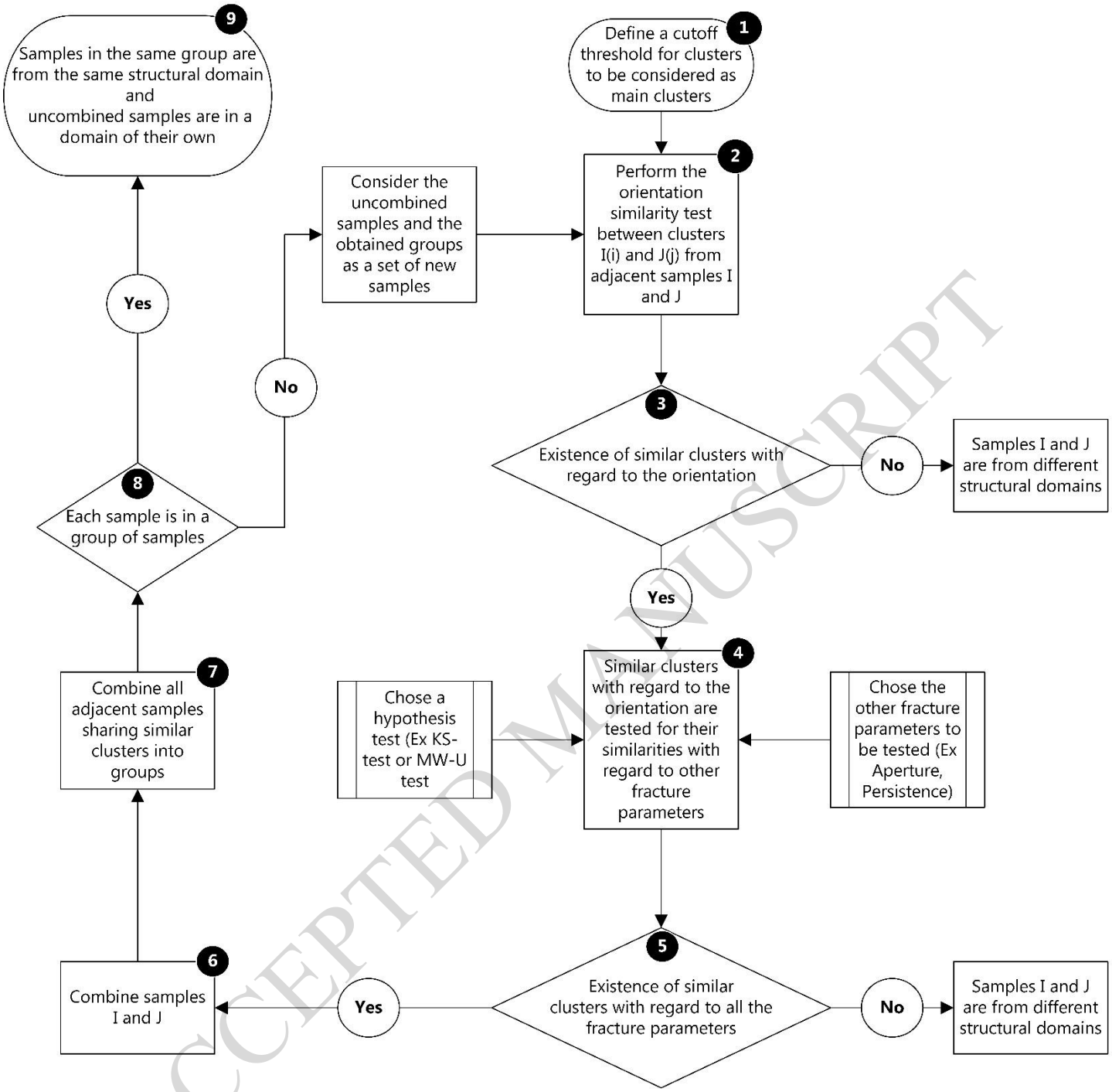

Figure 2: Flowchart for the multiparametric similarity test proposed in this study. The numbers in black circles indicate the steps in the flowchart.

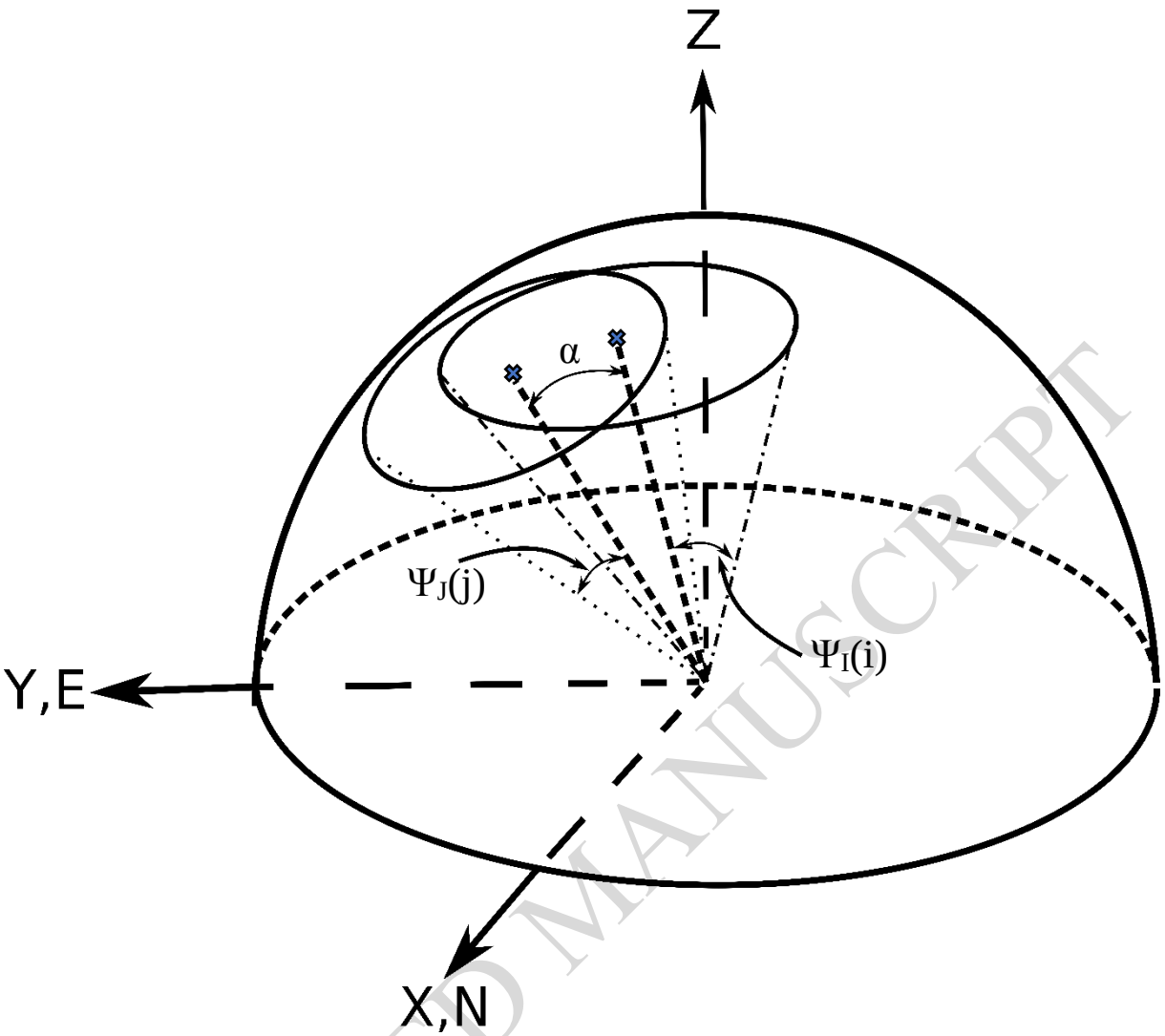

Figure 3: Illustration of the orientation similarity test via the comparison of the acute angle α and the means of a pair clusters and their cones of confidences $\Psi_{I(i)}$ and $\Psi_{J(j)}$ (modified after Mahtab and Yegulalp, 1984)

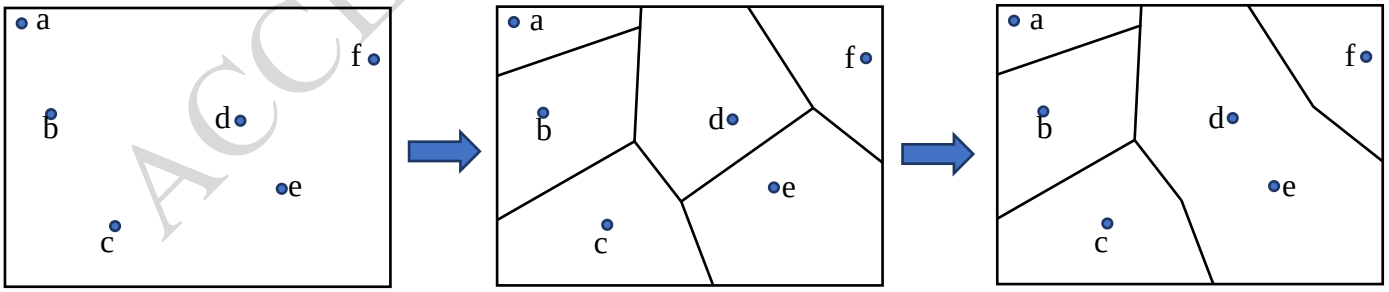

a) Fracture samples

b) Voronoi diagrams for each sample

c) Structural domain boundaries with samples **d** and **e** in the same domain

*Figure 4: Use of Voronoi diagrams in the delimitation of structural domain boundaries. From left to right, the maps represent, respectively, **a)** the fracture samples, **b)** the Voronoi diagrams for each sample, and **c)** the use of Voronoi diagrams for structural domain boundaries.*

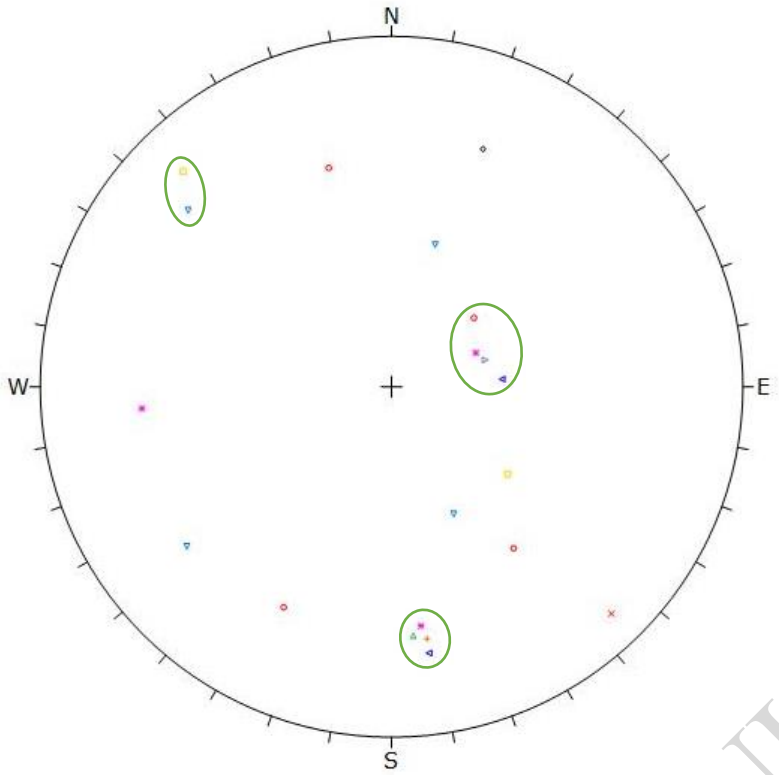

Figure 5: Identification of potential fracture clusters of adjacent samples for the similarity analysis on a stereonet. The circled poles of the cluster's resultants contain potentially similar clusters. Each geometrical form represents a sample which can have many clusters.

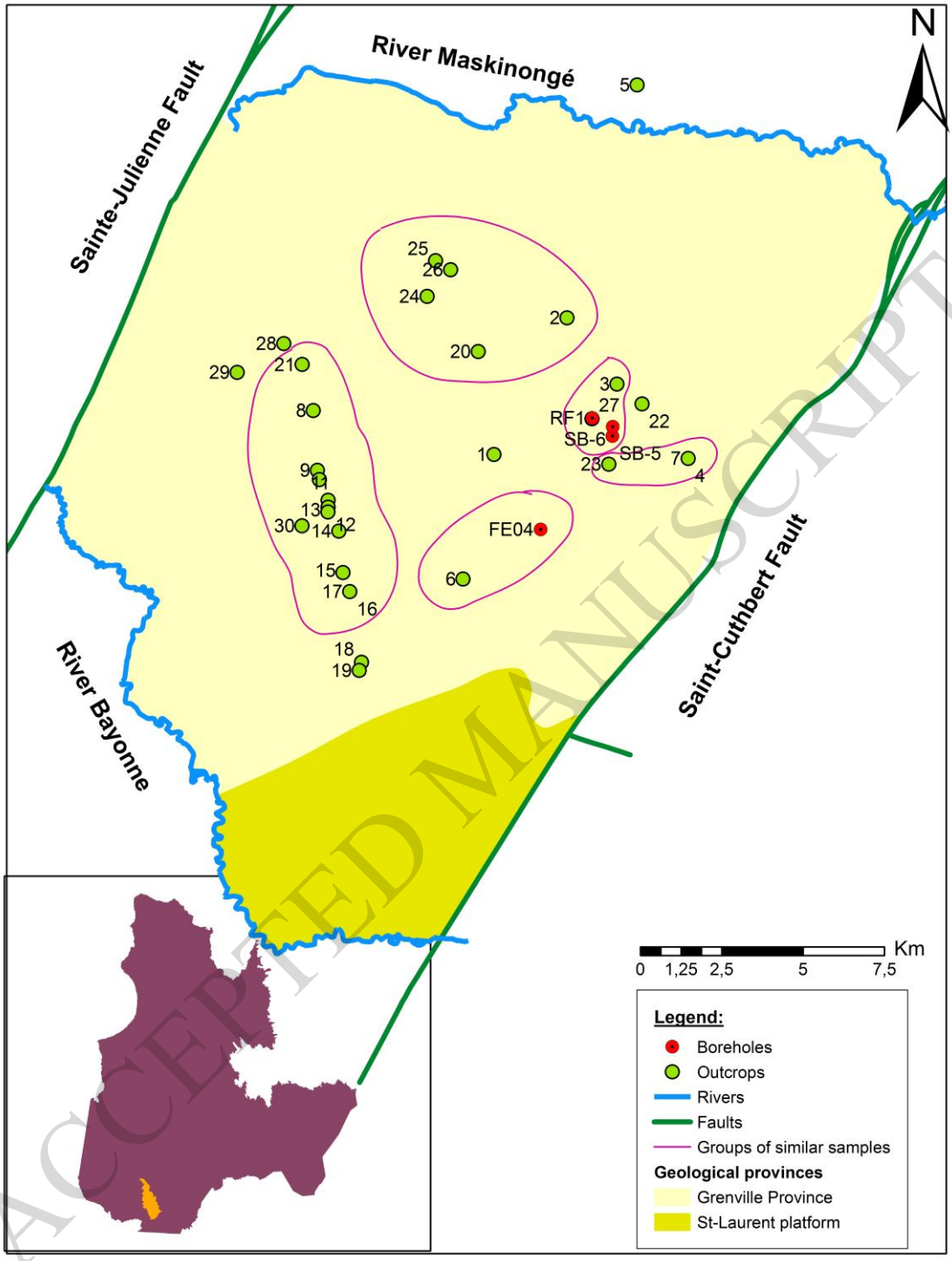

Figure 6: Grouping of fracture samples into structural domains according to their orientation similarities (Mahtab and Yegulalp's method). Circled samples are similar, and non-circled samples are not similar to any adjacent sample.

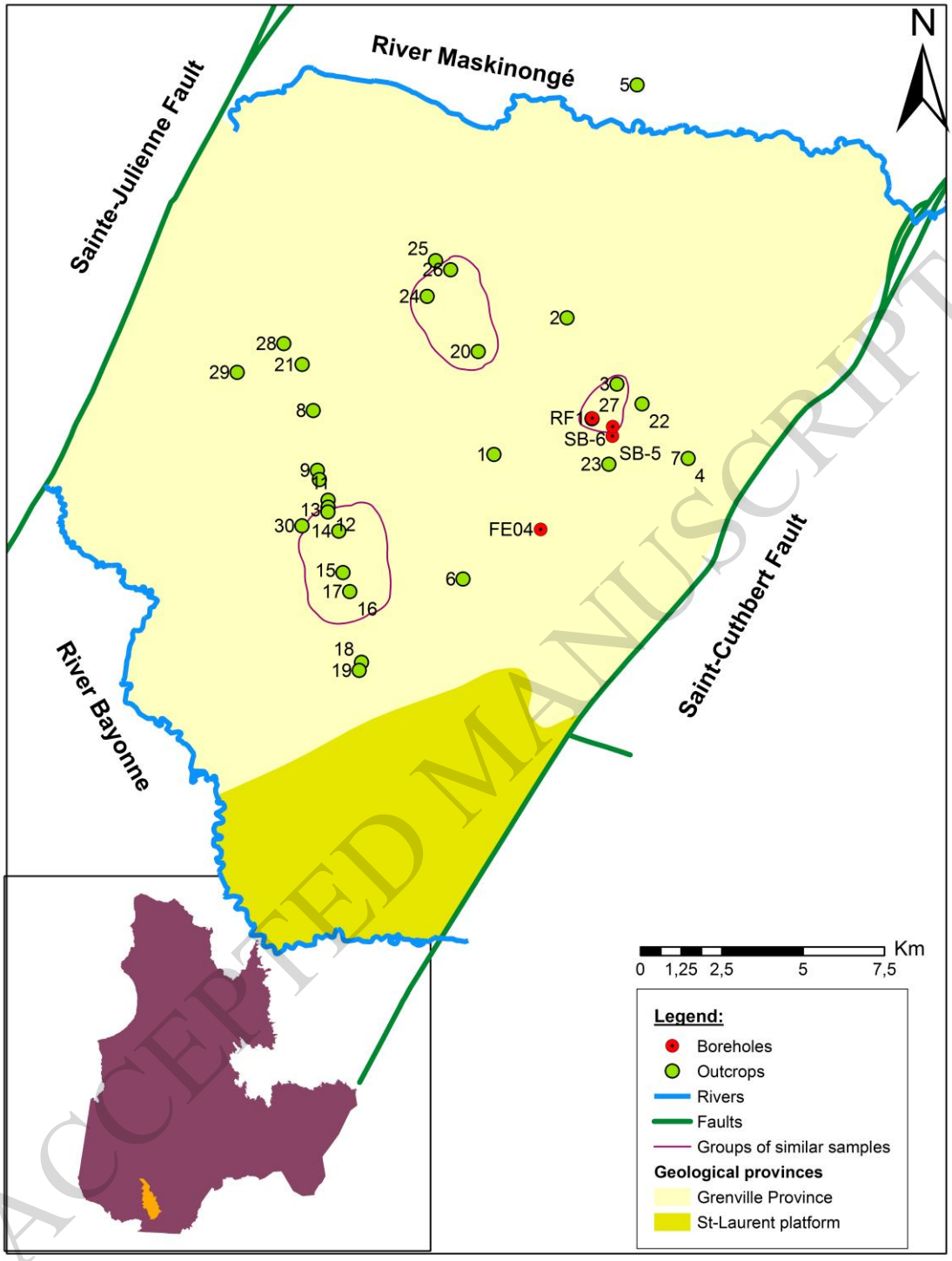

Figure 7: Grouping of fracture samples into structural domains according to their multiparametric similarities (fracture orientation, trace length, spacing, and aperture). Similar samples are circled, while non-circled samples are not similar to any adjacent sample.

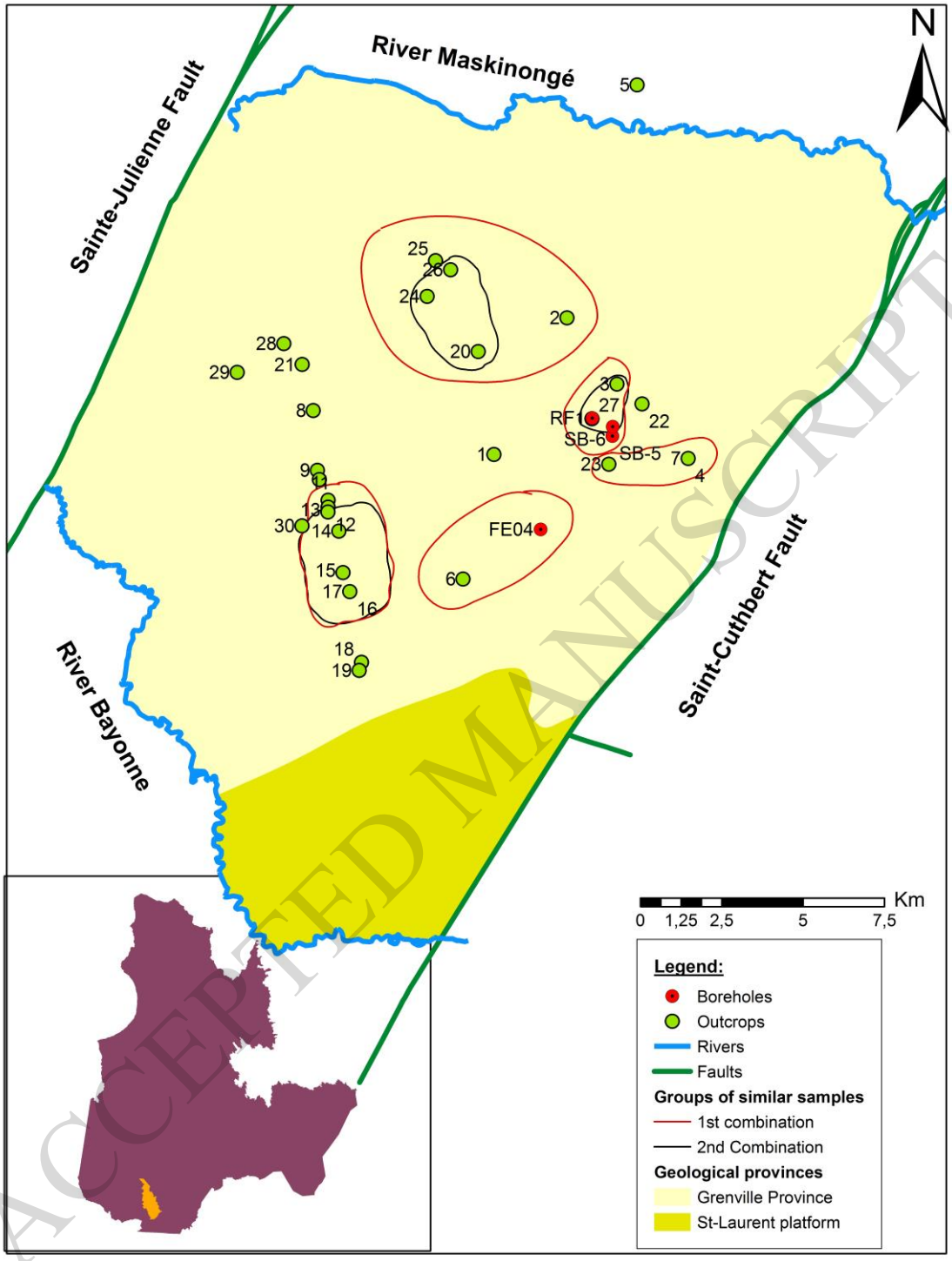

Figure 8: Grouping of fracture samples into structural domains according to their multiparametric similarities. Similar samples are circled, while non-circled samples are not similar to any adjacent sample. Red circles use fracture orientation and spacing, whereas black circles use fracture orientation, persistence, spacing, and apertures for the multiparametric similarity test.

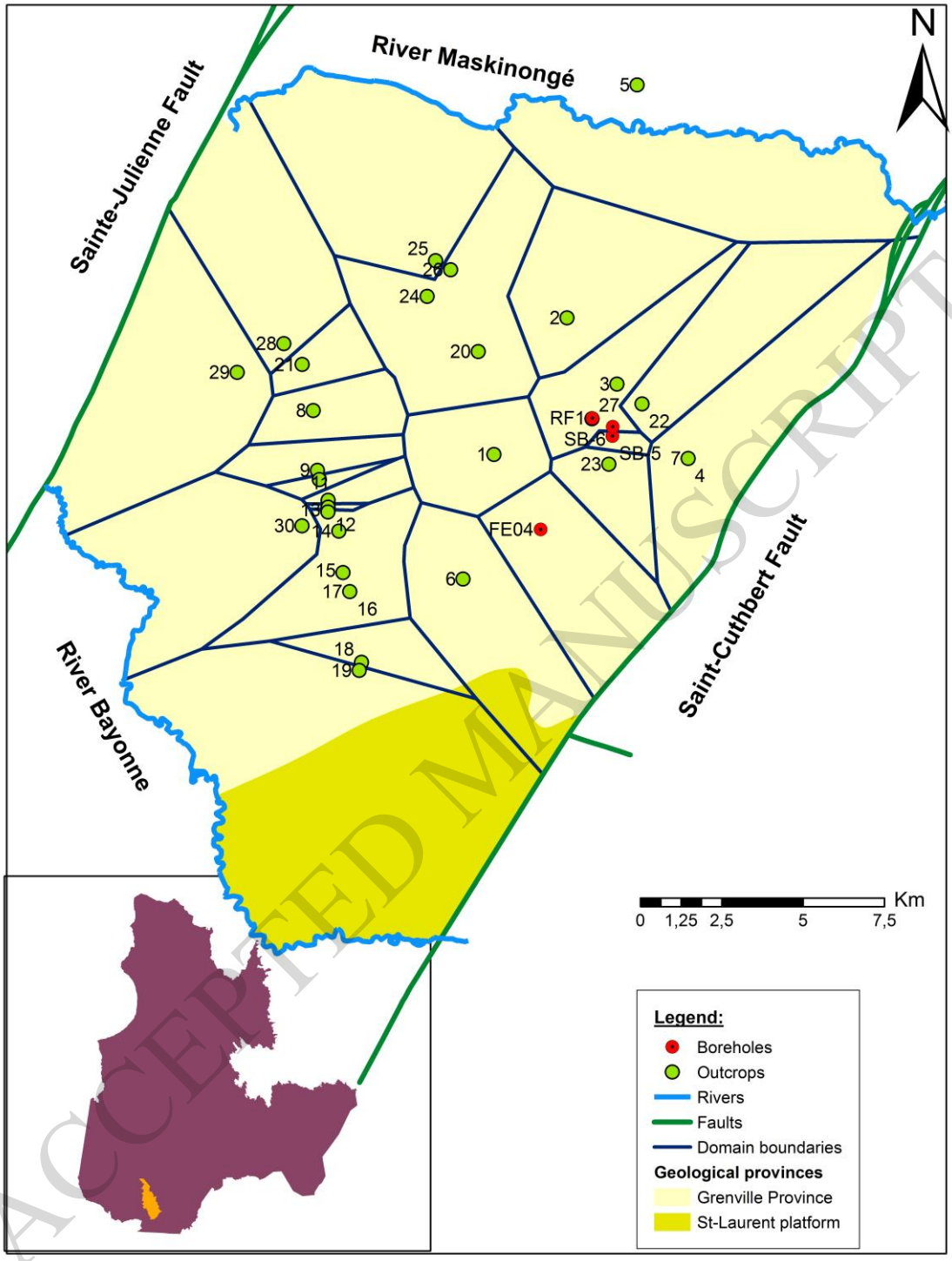

Figure 9: Use of Voronoi diagrams to delineate the domain boundaries according to the multiparametric similarity test, using fracture orientation, persistence, spacing, and aperture as fracture parameters.

Table 1: Partial results of the orientation similarity tests between clusters I(i) and J(j) respectively from adjacent samples I and J. R and FTR refer to reject and fail to reject, respectively.

Fracture sets I(i)–J(j)	Angle between I(i) and J(j)	Cone of confidence I(i)	Cone of confidence J(j)	Orientation Similarity test
2(1)–3(1)	22,6	11,7	7	R
27(2)–3(1)	4	15,2	7	FTR
22(1)–3(1)	36,3	6,2	7	R
22(1)–2(1)	22,1	6,1	11,7	R

Table 2: Partial results of the first iteration multiparametric similarity test using orientation, persistence, spacing, and aperture parameters. KS test and MW-U test refer to the Kolmogorov-Smirnov test and the Mann-Whitney U test. R and FTR stand for rejected and failed to be rejected. P-values in bold are higher than 0.05.

	Persistence-p values		**Spacing-p values**		**Aperture-p values**			
Fracture set I(i)–J(j)	**KS test**	**MW-U test**	**KS test**	**MW-U test**	**KS test**	**MW-U test**	**Orientation Similarity test**	**Overall Similarity**
27(2)–3(1)	**0,079**	**0,171**	**0,121**	**0,164**	**0,231**	**0,284**	FTR	FTR
23(1)–7(1)	0,042	0,027	**0,522**	**0,550**	2,8E-4	1,1E-5	FTR	R
20(2)–24(3)	**0,055**	**0,076**	**0,657**	**0,686**	**1,000**	**0,912**	FTR	FTR

Table 3: Second iteration similarity test using orientation, persistence, spacing, and aperture parameters. KS test and MW-U test refer to the Kolmogorov-Smirnov test and the Mann-Whitney U test. R and FTR stand for rejected and failed to be rejected. P-values in bold are higher than 0.05.

	Persistence-p values		Spacing-p values		Aperture-p values			
Fracture set I(i)–J(j)	**KS test**	**MW-U test**	**KS test**	**MW-U test**	**KS test**	**MW-U test**	**Orientation Similarity test**	**Overall Similarity**
G13(1)–12(1)	0,000	0,000	**0,785**	**0,761**	**0,853**	**0,738**	FTR	R
G13(2)–12(2)	0,021	**0,097**	**0,432**	**0,328**	**0,506**	**0,382**	FTR	R
G13(3)–30(2)	**0,253**	**0,136**	**0,954**	**0,477**	0,025	**0,093**	FTR	R
G20(4)–2(1)	**0,577**	**0,457**	**0,891**	**0,648**	0,000	0,000	FTR	R

Appendix C – Results of the orientation similarity tests between clusters

The results of the orientation similarity tests between clusters I(i) and J(j), respectively, from adjacent samples I and J are shown in the table below. R and FTR stand for rejected and failed to be rejected, respectively.

Fracture sets I(i)–J(j)	Angle between I (i) and J(j)	Cone of confidence I(i)	Cone of confidence J(j)	Orientation Similarity test
2(1)–3 (1)	22,6	11,7	7	R
27(2)–3 (1)	4	15,2	7	FTR
22(1)–3 (1)	36,3	6,2	7	R
22(1)–2 (1)	22,1	6,1	11,7	R
23(2)–4 (1)	27,3	7,2	7	R
23(2)–27 (2)	28,2	7,2	15,2	R
23(1)–7 (1)	13,15	7	13,3	FTR
23(2)–1 (1)	20,2	7,2	5,7	R
20(2)–24 (3)	4	7,2	7,8	FTR
25(1)–26 (2)	6	5,5	6,8	FTR
24(4)–26(1)	4,47	6,02	6	FTR
20(2)–25(1)	11,7	7,2	5,5	R
24(1)–2(1)	6,4	5,8	7	FTR
18(1)–19(1)	9,2	5,8	5,8	R
15(1)–19(1)	5	14,5	5,8	FTR
15(1)–18(1)	7,9	14,5	5,8	FTR
16(1)–17(1)	5,4	7,6	7,5	FTR
16(3)–6(1)	9	8,3	7,7	R

14(1)–16(5)	9,4	9,5	6,7	FTR
14(1)–17(2)	7	9,5	9,7	FTR
15(2)–16(1)	9	13,6	7,6	FTR
16(3)–18(1)	12	8,3	5,8	R
14(1)–13(1)	7,61	9,5	7	FTR
17(2)–13(1)	8,9	9,7	7	FTR
16(1)–13(2)	3	7,6	8,6	FTR
13(1)–1(1)	13,4	7	5,7	R
13(1)–12 (1)	5,1	7	5,6	FTR
14(1)–11 (1)	5,4	9,5	8,7	FTR
14(1)–12 (1)	4,4	9,5	5,6	FTR
12(1)–11 (1)	6	5,6	8,7	FTR
13(1)–30 (3)	16,1	7	3,8	R
12(4)–30 (2)	8	11,4	4,7	FTR
10(2)–30 (1)	4,2	7,3	3,8	FTR
11(2)–30 (5)	9,9	8,8	5	R
21(3)–28 (1)	10	7,8	6,3	R
8(1)–21 (3)	9,4	6,8	7,8	R
10(2)–8 (1)	3	7,3	6,8	FTR
21(3)–29 (2)	14,2	7,8	4,7	R
SB6(2)-3 (1)	3,1	7,7	6,9	FTR
SB6(2)–27 (2)	2,21	7,7	15,1	FTR
SB6(3)–RF1(1)	10	6,7	4,7	R
SB6(3)–SB5(1)	3,2	6,7	5,3	FTR
6(1)–FE04(1)	7	7,7	6,5	FTR

Appendix D – Results of the first iteration multiparametric similarity test

The results of the first iteration multiparametric similarity test, using fracture orientation, persistence, spacing and aperture parameters is shown in the table below. KS test and MW-U test refer to the Kolmogorov-Smirnov test and the Mann-Whitney U test. R and FTR stand for rejected and failed to be rejected, respectively. P-values in bold are higher than 0.05.

	Persistence-p values		Spacing-p values		Aperture-p values			
Fracture set I(i)–J(j)	**KS test**	**MW-U test**	**KS test**	**MW-U test**	**KS test**	**MW-U test**	**Orientation Similarity test**	**Overall Similarity**
27(2)–3 (1)	**0,079**	**0,171**	**0,121**	**0,164**	**0,231**	**0,284**	FTR	FTR
23(1)–7(1)	0,042	0,027	**0,522**	**0,550**	2,8 E-4	1,1E-5	FTR	R
20(2)–24(3)	**0,055**	**0,076**	**0,657**	**0,686**	**1,000**	**0,912**	FTR	FTR
25(1)–26(2)	0,018	0,020	**0,222**	**0,112**	**0,549**	**0,618**	FTR	R
24(4)–26(1)	**0,402**	**0,747**	**0,886**	**0,810**	**0,741**	**0,983**	FTR	FTR
24(1)–2(1)	**0,241**	**0,284**	**0,695**	**0,610**	0,001	0,002	FTR	R
15(1)–19(1)	5,6 E-5	6,8 E-5	1,3 E-5	1,3 E-4	0,006	0,001	FTR	R
15(1)–18(1)	2,4 E-5	7,8 E-5	4,9 E-4	0,001	0,003	0,001	FTR	R
16(1)–17(1)	**0,422**	**0,213**	**0,538**	**0,510**	**0,813**	**0,250**	FTR	FTR
14(1)–16(5)	**0,689**	**0,833**	**0,121**	**0,109**	**0,240**	**0,065**	FTR	FTR
14(1)–17(2)	**0,249**	**0,228**	**0,909**	**0,755**	**1,000**	**0,852**	FTR	FTR
15(2)–16(1)	**0,856**	**0,482**	**0,273**	**0,256**	**0,100**	**0,100**	FTR	FTR
14(1)–13(1)	**0,052**	**0,210**	**0,726**	**0,967**	**1,000**	**0,860**	FTR	FTR
17(2)–13(1)	**0,092**	**0,765**	**0,930**	**0,879**	**1,000**	**0,966**	FTR	FTR
16(1)–13(2)	**0,137**	**0,628**	**0,990**	**0,882**	0,045	**0,119**	FTR	R

13(1)–12(1)	9,3 E-7	4,8 E-5	**0,445**	**0,595**	**0,822**	**0,584**	FTR	R
14(1)–11(1)	**0,096**	**0,084**	**0,959**	**0,929**	**0,699**	**0,515**	FTR	FTR
14(1)–12(1)	3,6 E-5	3,4 E-4	**0,908**	**0,886**	**1,000**	**0,821**	FTR	R
12(1)–11 (1)	2,3 E-7	8,9 E-6	**0,301**	**0,331**	**0,398**	**0,187**	FTR	R
12(4)–30 (2)	5,0 E-3	4,7 E-2	**0,075**	0,035	0,043	0,046	FTR	R
10(2)–30 (1)	**0,234**	**0,917**	0,013	**0,056**	0,044	**0,161**	FTR	R
10(2)–8 (1)	0,000	0,000	0,005	0,009	**0,083**	**0,280**	FTR	R
SB6(2)–3 (1)			**0,617**	**0,267**	0,032	**0,149**	FTR	R
SB6(2)–27 (2)			**0,573**	**0,665**	**1,000**	**1,000**	FTR	FTR
SB6(3)–SB5(1)			**0,314**	**0,207**	0,022	0,022	FTR	R
6(1)–FE04(1)			**0,227**	**0,197**	0,010	0,049	FTR	R

Appendix E –Fracture clusters and fracture characteristics of structural domains.

The fracture clusters and fracture characteristics of structural domains obtained by the multiparametric similarity test using fracture orientation, persistence, spacing, and aperture parameter. The characteristics of structural domains correspond to the compartmentalization illustrated in Figure 9.

	Compartments	Clusters	Dip (°)	Dip direction (°)	Persistence (m)	Aperture (mm)	Spacing (m)
Groups of samples	**G3**	1	35±18	267±18	2─6	0,1─0,1	0,3─1,4
		2	75±18	352±18	1─5	0,1─3	0,1─4,5
	G13	1	87±21	207±21	0,5─4	0,1─2	0,1─9
		2	86±19	246±19	0,5─4	0,1─4	0,1─8
		3	88±20	134±20	0,5─4	0,1─3	0,2─5
		4	17±25	331±25	0,8─4	0,1─3	1,4─3,4
	G20	1	89±21	191±21	0,6─6	0,1─0,1	0,1─5
		2	74±18	43±18	0,5─4	0,1─2	0,1─3
		3	31±22	253±22	0,8─6,5	0,1─0,1	0,1─1
		4	84±10	164±10	0,5─6,2	0,1─0,1	0,1-2
Uncombined samples	**1**	1	72±10	201±10	1,5─5		0,2 ± 2,2
	2	1	89±17	306±17	1─3	1─3	0,1─2
	4	1	77±13	174±13	0,4─1,5	0,1─2	0,1─1,2
	5	1	70±23	171±23	0,6─4	1─3	0,2─3
		2	8±27	311±27	1─4	0,1─2	0,3─1
	6	1	73±19	133±19	1─5	0,1─1	0,1─5
		2	46±14	198±14	1─2	0,1─0,1	2,3─4,7
		3	43±21	334±21	1,5─3	0,1─2	0,4─0,8
		4	74±12	51±12	1,5─2	0,1─1	0,3─0,3
	7	1	84±19	278±19	0,5─1,5	0,5─2	0,3─1,3
	8	1	89±27	177±27	0,15─2	0,1─2	0─2,2
		2	80±24	250±24	0,3─1,8	0,1─2	0,4─3
		3	46±18	175±18	0,5─2	1─1	0,3─5
		4	51±11	6±11	0,15─1,5	0,1─1	0,7─6
	9	1	46±6	50±6	1,2─4	0,1─2	1,6─7
		2	3±29	245±29	1,5─5	0,1─2	0,2─1,7
	10	1	5±17	146±17	1,7─8	1─2	2,7─8,7
		2	90±22	180±22	0,7─4	0,1─2	0,1─7,4
		3	87±4	260±4	1,8─3	2─2	3,4─3,4
	11	1	88±27	22±27	0,5─2,5	0,1─1	0,1─6
		2	79±20	266±20	0,6─2	0,1─1	0,1─3,4

		3	16±17	328±17	2,5─4	1─2	2─3
	12	1	90±20	207±20	0,5─7,5	0,1─2	0,1─8
		2	83±18	242±18	0,3─4	0,1─3	0,3─4,2
		3	5±20	291±20	0,5─6	0,1─3	0,5─9,8
		4	84±23	328±23	1─4	0,1─2	0,7─7
	18	1	83±15	148±15	0,5─1,8	0,1─1	0,1─1,6
		2	81±20	359±20	0,5─2	0,1─2	0,15─1,4
		3	87±20	45±20	0,2─2	0,1─2	0,1─5
	19	1	31±20	182±20	0,2─2	0,1─1	0,03─1,9
	21	1	89±21	61±21	0,8─3	0,1─2	0,13─4,5
		2	78±15	32±15	0,5─3	0,1─3	0,1─7,4
		3	82±20	3±20	0,7─3	0,1─2	0,1─5,13
	22	1	83±20	316±20	0,7─8	0,1─0,1	0,01─1,8
	23	1	82±23	101±23	0,5─20	0,1─2	0,03─1,4
		2	87±23	18±23	1─20	0,1─0,1	0,03─2,4
	25	1	86±20	36±20	1─17	0,1─60	0,05─2,7
	28	1	87±21	18±21	0,34─6	0,1─30	0,14─3,15
		2	80±18	239±18	0,7─4	0,1─1,5	0,85─14,9
		3	17±25	211±25	1,2─18,2	0,1─2	0,6─8
	29	1	88±20	289±20	0,25─5	0,1─10	0,02─5,3
		2	73±23	13±23	0,25─3	0,1─40	0,02─3,5
	30	1	87±23	1±23	0,6─8,6	0,1─10	0,08─16,9
		2	89±27	130±27	0,45─12	0,1─10	0,01─15,3
		3	90±27	47±27	0,3─4,5	0,1─10	0,02─11,2
		4	24±27	244±27	1,75─10,8	0,1─200	0,4─35,6
		5	87±22	270±22	0,5─4,5	0,1─10	0,04─19
	SB5	1	31±19	254±19		0─249	0,03─5,9
	RF1	1	34±23	230±23		0─68	0,02─11,27
		2	70±22	26±22		0─0	0,04─7,38
		3	66±25	164±25		0─73	0,01─4,53
		4	60±23	323±23		0─214	0,02─7,45
	FE04	1	13±28	253±28		0─15	0,01─3,03
		2	65±18	314±18		0─12	0,01─3,05